arXiv:1210.5948v1 [math.GT] 22 Oct 2012

VANISHING CYCLES AND HOMOTOPIES OF WRINKLED FIBRATIONS

STEFAN BEHRENS AND KENTA HAYANO

Abstract. Wrinkled fibrations are certain smooth maps from 4–manifolds to surfaces. To a wrinkled fibration one can associate its base diagram and its vanishing cycles. While it is rather well understood how the base diagram evolves under homotopies between wrinkled fibrations, the behavior of the vanishing cycles is less obvious. We study this problem for merge homotopies and give various applications.

1. Introduction

Wrinkled fibrations are certain smooth maps from 4–manifolds to surfaces.[1] They are natural generalizations of (broken) Lefschetz fibrations. In fact, they were introduced into 4–manifold topology in this precise context [B1, L] and have been attracting independent interest ever since. Right from the beginning, people have also studied certain homotopies between wrinkled fibrations which were exploited in order to construct other types of maps with desired properties.

In order to motivate the results of the present paper, we use an analogy with Morse theory. It is well known that a generic smooth map to a 1–dimensional target is a Morse function which is injective on its critical points. Similarly, generic maps to 2–dimensional targets exhibit only two types of singularities, folds and cusps, their critical locus is 1–dimensional and is mapped into the target as regularly as possible. Wrinkled fibrations form a subset of these generic maps and are analogous to Morse functions without local extrema.

A Morse function is essentially determined by its set of critical values, the topology of the regular level sets and certain framed spheres in the level sets just below a critical value that control how the level set is changed when passing the critical level. (In the case of real valued Morse functions this data is basically equivalent to a handle decomposition of the underlying manifold.) In generic homotopies between Morse functions the above mentioned structures evolve in well understood ways.

For wrinkled fibrations we find a similar situation. The set of critical values, henceforth called the *critical image*, divides the base surface into connected regions. The base surface decorated with the critical image and the topological type of the regular fibers over the various regions is commonly referred to as the *base diagram*. In order to determine the wrinkled fibration one has to know certain simple closed curves in the regular fibers known as the *(fold) vanishing cycles* which encode how the topology changes when one crosses the critical image. In many interesting cases the knowledge of the base diagram and the vanishing cycles suffices. For more details we refer to [GK2].

While it is rather well understood how the base diagram evolves in homotopies between wrinkled fibrations, the behavior of the vanishing cycles is still largely mysterious. The main problem is the following. In the course of a homotopy, two formerly disconnected regions in the base diagram can be joined. As a result, the two sets of vanishing cycles appear in a single surface and it turns out that the way they appear depends on the homotopy. This phenomenon is caused by two kinds of homotopies known as R_2*-moves* and *merge homotopies.* The former have been studied in [H2] and the latter are the main focus of the present paper.

---

[1] Wrinkled fibrations have many different names in the literature. To name a few: *purely wrinkled fibrations*, *indefinite Morse 2-functions*, *indefinite stable maps*, *indefinite generic maps.*

We now give a section by section outline of the paper. In Section 2 we recall the definitions of and some facts about wrinkled fibrations and their homotopies and we introduce our main technical tool, *horizontal distributions*, which provide a notion of parallel transport in wrinkled fibrations. We also discuss simple wrinkled fibrations and their (surgered) surface diagrams which were introduced by Williams [W1, W2].

The technical core of this paper is Section 3 where we discuss merge homotopies. We begin by describing merge homotopies in terms of local models and pin down the necessary geometric structures to embed the models. Then we relate these structures to the parallel transport after the homotopy and obtain an interpretation in terms of mapping class groups of the fibers.

In Section 4 we apply our results to the uniqueness problem for surface diagrams. According to Williams [W2], any two homotopic simple wrinkled fibrations can be related by a sequence of four basic deformations known as *handleslide*, *multislide*, *shift* and *stabilization.* We obtain a concrete description in terms of mapping class groups of how surface diagrams can be changed by multislides (Proposition 4.1) and by what we call *generalized shifts* (Proposition 4.2). Together with the results from [H2], which we briefly review, this completes the description of Williams' moves for surface diagrams in terms of mapping class groups.

In Section 5 we consider some constructions of simple wrinkled fibrations involving cusp merge homotopies and show how to obtain the resulting surface diagrams. We show how to construct surface diagrams for Lefschetz fibrations out of the (Lefschetz) vanishing cycles. As an example, we obtain genus two surface diagrams for the elliptic surfaces $E(n)$. Furthermore, given a closed, oriented 3–manifold M we show how to obtain surface diagrams for $S^1 \times M$ from a Heegaard diagram of M. As examples, we give a new surface diagram of $S^1 \times S^3$ and $S^1 \times L(p, 1)$. It is interesting to note that these diagrams come from simple wrinkled fibrations over S^2 which are necessarily homotopic to a constant map. As a consequence, the diagrams are not related by Williams' moves to the previously known ones which were derived from certain homotopically non-trivial bundle projections. Finally, we discuss the *(boundary) fiber sum* construction for simple wrinkled fibrations and show how it can be interpreted in terms of surface diagrams.

2. WRINKLED FIBRATIONS AND THEIR HOMOTOPIES

We are interested in certain maps from 4-manifolds to surfaces and homotopies between them. The maps are defined by the structure of their singularities as follows. To state the conditions let X be a 4-manifold, B a surface and $f\colon X \to B$ a smooth map. We always assume that both X and B are oriented, that f is surjective and satisfies $\partial X = f^{-1}(\partial B)$. The latter condition implies that the regular fibers of f are closed, orientable surfaces and we will fix orientations according to the fiber first convention[2]. Moreover, we require the *critical locus* of f, which we denote by

$$\mathcal{C}_f = \big\{p \in X \,\big|\, \mathrm{rk}(df_p) < 2\big\},$$

---

[2] Around a regular point we can choose orientation preserving coordinates such that f looks like the map $\mathbb{R}^2 \times \mathbb{R}^2 \to \mathbb{R}^2$ given by the projection onto the second factor. The first factor corresponds to the fibers and naturally inherits an orientation.

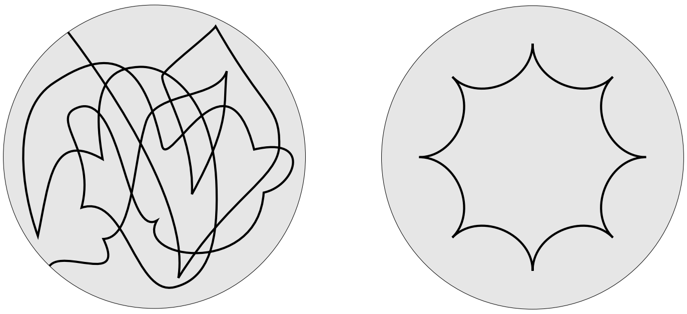

Figure 1. Examples of critical images of a wrinkled fibration (left) and a simple wrinkled fibration (right) over the disk.

to consist only of *indefinite folds and cusps*. These singularities can be characterized in terms of the local models

$$\begin{aligned} \mathrm{F}(t,x,y,z) &= \big(t,\, x^2+y^2-z^2\big) \\ \mathrm{C}(t,x,y,z) &= \big(t,\, x^3+3tx+y^2-z^2\big) \end{aligned} \tag{2.1}$$

where F and C stand for fold and cusp, respectively. We then say that f has an indefinite fold or cusp singularity at $p \in X$ if there are coordinate charts centered at $p \in X$ and $f(p) \in B$, so called *model coordinates*, in which f is given by the respective model map. For convenience, we will always assume that model coordinates respect the orientations of X and B; this is no restriction since both models are invariant under the orientation reversing diffeomorphism $(t,x,y,z) \mapsto (t,x,y,-z)$. Since we will not encounter any definite singularities we will drop the adjective indefinite from now on and simply speak of folds and cusps.

From the local models it is easy to see that folds come in 1-dimensional families while each cusp is isolated and surrounded by two arcs of folds. At times we will be sloppy and refer to both, critical points and critical values, as fold or cusp points. However, it will be clear from the context whether we are working on the source or the target space.

Finally, we impose some genericity assumptions on f. In detail, this means that all cusp points of f are contained in the interior of X, that f is injective on the preimage of the images of the cusp points and that the restriction of f to its fold points is a generic immersion, that is the fold arcs in B have only simple crossings in the interior of B and meet the boundary of B transversely. (The last condition implies that f restricts to a circle valued Morse function over each boundary component of B.) Following the terminology of [B3] we make the following definition.

Definition 2.1. A smooth map $f\colon X \to B$ with the above properties is called a *wrinkled fibration* with *total space* X and *base* B. The *fiber* of f over $b \in B$ is the preimage $f^{-1}(b)$. We say that f is a *simple wrinkled fibration* if, in addition, its critical locus $\mathcal{C}_f$ is connected, is contained in the interior of X, contains at least one cusp, f is injective on $\mathcal{C}_f$ and all (regular) fibers are connected.

The set of critical values of a wrinkled fibration, called the *critical image*, is an immersed collection of circles with finitely many cusps and transverse intersection between fold arcs. A typical example is shown in Figure 1. Although classically known to singularity theorists, wrinkled fibrations became relevant in the 4–dimensional context through the work of Baykur and Lekili [B1, L]. Soon after, simple wrinkled fibrations were introduced by Williams[3] [W1] who also proves the following existence result.

Theorem 2.2 (Williams [W1])**.** *Let* X *be a closed, oriented 4–manifold. Then any continuous map* $X \to S^2$ *is homotopic to a simple wrinkled fibration of arbitrarily high fiber genus.*

Another theorem of Williams [W1] addresses the structure of homotopies between wrinkled fibrations and settles a conjecture of Lekili [L]. The theorem states that there is a finite set of basic deformations such that any two homotopic wrinkled fibrations can be related by a finite sequence of these deformations. For more details about the deformations we refer the reader to [L, W1] as well as [GK1] which contains a detailed account on existence and uniqueness theorems for wrinkled fibrations. In the present paper we will focus on one particular type of deformation, namely merge homotopies, starting with Section 3.

2.1. **Horizontal distributions and parallel transport.**

The critical image of a wrinkled fibration divides the base into various (connected) regions over which the map restricts to a proper submersion. Standard arguments in differential topology then show that different fibers over the same region must be diffeomorphic. Diffeomorphisms are obtained by generalizing the concept of parallel transport in vector bundles which involves two choices: a path in the base connecting the images of the fibers and some kind of connection. We will further generalize the concept of parallel transport to the context of wrinkled fibrations, our approach is inspired by Ehresmann's notion of connection for fiber bundles and by the notion of gradient-like vector fields for Morse functions which can be considered as connections. Similar constructions have already been used in this context by the second author [H2].

Definition 2.3. Let $f\colon X \to B$ be a wrinkled fibration. The collection of subspaces $\mathcal{V}_f := \ker(df) \subset TX$ is called the *vertical distribution* of f. A *horizontal distribution* for f is a collection of subspaces $\mathcal{H} \subset TX$ such that

(i) at each point $p \in X$ there is a splitting $T_pX = (\mathcal{V}_f)_p \oplus \mathcal{H}_p$ and
(ii) near a critical point there are model coordinates such that $\mathcal{H}$ corresponds to the Euclidean orthogonal complement of the vertical distribution of the model singularity (F or C, see (2.1)).

At a regular point $p \in X$ the vertical space $(\mathcal{V}_f)_p$ is just the tangent space of the fiber containing p. However, at critical points the rank of $\mathcal{V}_f$ jumps so that neither $\mathcal{V}_f$ nor any complementary $\mathcal{H}$ are sub-bundles of TX unless f is a submersion. Nevertheless we can speak of sections of $\mathcal{V}_f$ and $\mathcal{H}$.

Remark 2.4. It is easy to see that the space of horizontal distributions is nonempty, for example by choosing an appropriate Riemannian metric that is compatible with some model coordinates. It would be desirable if the space of horizontal distributions were connected or even contractible. However, this is not obvious since the homotopy type of the spaces of model coordinates around the critical points might be nontrivial. Alternatively, we might have defined horizontal distributions simply as orthogonal complements of the vertical distribution with respect to to arbitrary Riemannian metrics, which would give a contractible space of horizontal distributions. The drawback of this approach is that we could not investigate the dynamics of horizontal distributions near critical points purely in terms of the local models.

---

[3] who used the term *simplified purely wrinkled fibrations*

Given a wrinkled fibration $f\colon X \to B$, we will call a curve $\tilde{\gamma}\colon [0,1] \to X$ *horizontal* if it is nowhere tangent to a fiber of f, that is, if its tangent vector $\dot{\tilde{\gamma}}(t)$ is not contained in $\mathcal{V}_f$ for any value of t. Furthermore, if $\mathcal{H}$ is a horizontal distribution for f and $\tilde{\gamma}$ is everywhere tangent to $\mathcal{H}$, then $\tilde{\gamma}$ is called *$\mathcal{H}$–horizontal.* Note that $\mathcal{H}$–horizontal curves are always horizontal while the converse does not hold. To obtain a notion of parallel transport we need to study the dynamics of horizontal distribution. This turns out to be very similar as in the case of gradient like vector fields. The following is a more or less straightforward consequence of the existence and uniqueness theory for ordinary differential equations.

Proposition 2.5. *Let $f\colon X \to B$ be a wrinkled fibration, $\mathcal{H}$ a horizontal distribution for f and $\gamma\colon [0,1] \to B$ an embedded arc such that $\gamma(0)$ and $\gamma(1)$ are regular values. For any pair (t,p) where $t \in [0,1]$ and $p \in \Sigma_t = f^{-1}(\gamma(t))$ is a regular point of f there is a unique $\mathcal{H}$–horizontal lift $\tilde{\gamma}_{t,p}\colon I_{t,p} \to X$ of γ defined on a maximal open interval $I_{t,p} \subset [0,1]$ containing t. Furthermore, the curves $\tilde{\gamma}_{t,p}$ have left and right limits in X which are contained in either Σ_0, Σ_1 or $\mathcal{C}_f$.*

Given a pair (t,p) as above we say that $\tilde{\gamma}_{t,p}$ *runs into $\mathcal{C}_f$* (resp. *emerges from $\mathcal{C}_f$*) if its left (resp. right) limit is contained in $\mathcal{C}_f$. We define the *vanishing sets* of γ as

$$V_0^{\mathcal{H}}(\gamma) := \big\{p \in \Sigma_0 \big|\, \tilde{\gamma}_{0,p} \text{ runs into } \mathcal{C}_f\big\}$$
$$V_1^{\mathcal{H}}(\gamma) := \big\{q \in \Sigma_1 \big|\, \tilde{\gamma}_{1,q} \text{ emerges from } \mathcal{C}_f\big\}$$

and it follows from Proposition 2.5 that we obtain a diffeomorphism

$$\mathrm{PT}_\gamma^{\mathcal{H}}\colon \Sigma_0 \setminus V_0^{\mathcal{H}}(\gamma) \to \Sigma_1 \setminus V_1^{\mathcal{H}}(\gamma)$$

by sending $x \in \Sigma_0$ to $\tilde{\gamma}_{0,x}(1) \in \Sigma_1$. We will refer to $\mathrm{PT}_\gamma^{\mathcal{H}}$ as the *parallel transport* along γ with respect to $\mathcal{H}$. We describe the three most important special cases of this construction.

Example 2.6 (Arcs of regular values)**.** If γ does not meet any critical values of f, then its image is entirely contained in one component of $B \setminus f(\mathcal{C}_f)$ over which f is a proper submersion. In this situation the vanishing sets are empty and we recover the usual notion of parallel transport in fiber bundles. Furthermore, standard arguments show that the isotopy class of the parallel transport diffeomorphism does not depend on the horizontal distribution and only depends on the homotopy class of γ (as a map into $B \setminus f(\mathcal{C}_f)$) relative to its endpoints. (Note that the space of model coordinates mentioned in Remark 2.4 is not an issue here.)

Example 2.7 (Crossing a fold arc)**.** Next, we assume that the endpoints of γ lie in adjacent regions and γ crosses the critical image exactly once and transversely in a fold point. The model of the fold singularity implies that the composition $\gamma^{-1} \circ f\colon f^{-1}\big(\gamma([0,1])\big) \to [0,1]$ is a Morse function with one critical point of index 1 or 2 depending on the direction in which γ crosses the fold arc. It is easy to see that the vanishing set over one endpoint is a simple closed curve and a pair of points over the other. The simple closed curve is also called *(fold) vanishing cycle* of f associated to γ and $\mathcal{H}$. We denote the fiber over $\gamma(0)$ by Σ and assume that it contains the vanishing cycle $c \subset \Sigma$. Similarly we denote the fiber over $\gamma(1)$ by Σ' and the vanishing set consists of two points $\{p,q\} \subset \Sigma'$. By parallel transport we thus obtain a diffeomorphism

$$\mathrm{PT}_\gamma^{\mathcal{H}}\colon \Sigma \setminus c \to \Sigma' \setminus \{p,q\}$$

which maps a tubular neighborhood of c with c removed to two disjoint punctured disks around p and q. On one hand this allows us to identify Σ' with the surface obtained by surgery on Σ along c, on the other hand we can also identify Σ with

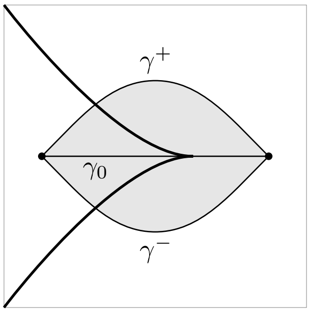

Figure 2. Parallel transport near a cusp

the surgery on Σ' along the 0–sphere $\{p, q\}$. The latter observation will become important later on.

Example 2.8 (Crossing a cusp)**.** Finally, we consider the situation when γ connects two adjacent regions through a cusp. An investigation of the cusp model shows that the vanishing set on one side is a single point while on the other side it is the union of two simple closed curves that intersect transversely in one point. We will also refer to these curves as *vanishing cycles* (this choice of terminology is justified below). With similar notation as in the previous example we obtain a parallel transport diffeomorphism

$$\mathrm{PT}^{\mathcal{H}}_{\gamma}\colon \Sigma \setminus (c^+ \cup c^-) \to \Sigma' \setminus \{p\}$$

where $c^\pm \subset \Sigma$ are the vanishing cycles and $p \in \Sigma'$ is the point. As in the second example, there is a surgical interpretation, albeit a slightly less familiar one. Note that a closed regular neighborhood of the union $c^+ \cup c^-$ is diffeomorphic to a one-holed torus. If we remove the interior of such a neighborhood and fill the resulting boundary component with a disk, then we obtain a closed surface known as the *symmetric surgery* on (or *contraction* of) Σ along c^+ and c^-. Arguing as above, we can use $\mathrm{PT}^{\mathcal{H}}_{\gamma}$ to identify Σ' with the symmetric surgery on Σ.

Remark 2.9. A cusp is the common limit of two arcs of folds. As a consequence, there are two different ways to consider the Example 2.8 above as a limit of Example 2.7. As we will see, this observation equips the fiber over the endpoint of an arc as in Example 2.8 whose vanishing set is a point with two complementary tangent directions at this point.

To make this precise, we take a one parameter family of arcs γ_t, $t \in [-1, 1]$, with common endpoints such that they trace out a disk as shown in Figure 2 and that γ_0 fits Example 2.8 while all the others fit Example 2.7. For $t \neq 0$ we denote the vanishing sets associated to γ_t by $c_t \subset \Sigma$ and $\{p_t, q_t\} \subset \Sigma'$ and for γ_0 we denote them by $c_0^+ \cup c_0^- \subset \Sigma$ and $p_0 \in \Sigma'$. For convenience we let $\gamma^\pm = \gamma_{\pm 1}$ and define $c^\pm$ and $\{p^\pm, q^\pm\}$ analogously. One can show what the notation suggests, namely that the curves $c^\pm$ are isotopic to $c_0^\pm$; the isotopies are given by c_t as t goes to zero from below and above. By choosing the horizontal distribution carefully one can actually assume that $c_t = c_0^\pm$ where the superscript sign agrees with the sign of t which we shall henceforth do. Furthermore, as t goes to zero from below and above one can show that the points p_t and q_t all converge to p_0 tracing out an embedded arcs $A^\pm$ in Σ' from p^+ to q^+, resp. from p^- to q^-. These arcs meet transversely in p_0 and thus specify the afore-mentioned tangent directions in $T_{p_0}\Sigma'$. Note that there is another way to obtain two such arcs, namely we can map $c^\mp \setminus c^\pm$ into Σ' using $\mathrm{PT}^{\mathcal{H}}_{\gamma^\pm}$ and take the closure. As with the vanishing cycles one can show that these arcs are isotopic relative to their endpoints to $A^{\pm}$ and again one can assume that they actually agree.

2.2. **Surface diagrams and surgered surface diagrams.** We now shift our attention from general wrinkled fibrations to simple wrinkled fibrations over the sphere or the disk. We denote these maps by $w\colon X \to S$, $S \in \{S^2, D^2\}$, and when the base surface is a disk we will always assume that its boundary is contained in the lower genus region.[4] Following Williams [W1] one can assemble all the fold vanishing cycles of such a simple wrinkled fibration in a higher genus fiber to obtain a combinatorial description reminiscent of a Heegaard diagram.

Definition 2.10. A *surface diagram* $\mathfrak{S} = (\Sigma; c_1, \dots, c_l)$ consists of a closed, oriented surface Σ and a cyclically ordered collection of at least two simple closed curves $c_i \subset \Sigma$, called *vanishing cycles*, such that any pair of adjacent curves c_i and c_{i+1} (where $l + 1 = 1$) has geometric intersection number[5] one.

It is also customary to denote the collection of vanishing cycles by $\Gamma = (c_1, \dots, c_l)$ but we will not make use of this notation in the present paper.

Remark 2.11. There are good reasons to assume that a surface diagram contains at least two vanishing cycles as explained in [B3]. Although fake surface diagrams with only one vanishing cycle are also useful in some situations, they exhibit pathological behavior.

The procedure to obtain a surface diagram from a simple wrinkled fibration has been explained many times before so we shall be brief. However, we would like to point out that certain choices are involved that have been made implicitly in the previous literature. For a given simple wrinkled fibration $w\colon X \to S$ these are:

1. a reference point in the higher genus region,
2. a collection of *reference arcs*, that is, curves in S as in Example 2.7 that start at the reference point and are otherwise disjoint such that there is exactly one reference arc for each fold arc of w and
3. a horizontal distribution for w.

The vanishing cycles for the reference arcs then form a surface diagram. Observe that for an arbitrary choice of these data the vanishing cycles might not be in general let alone minimal position. However, both of these properties can be achieved by changing the horizontal distribution. Indeed, it is easy to see that one can modify the horizontal distribution with the effect that one vanishing cycle is changed by an arbitrary isotopy of the reference fiber while all others remain unchanged. In the following we will tacitly assume that the vanishing cycles in surface diagrams are in general position.

A natural notion of *equivalence of surface diagrams* is generated by cyclic permutations of the vanishing cycles, separately isotopies to single vanishing cycles in the surface as well as mapping the whole configuration into a (possibly different) surface with an orientation preserving diffeomorphism. The properties of parallel transport imply that the surface diagram of a simple wrinkled fibration w is well defined up to equivalence.

It is known that equivalence classes of surface diagrams are in one-to-one correspondence with equivalence classes of simple wrinkled fibrations over the disk, where two such simple wrinkled fibrations $w\colon Z \to D^2$ and $w'\colon Z \to D^2$ are said to be equivalent if there is a commutative diagram

---

[4] The German word for disk is “Scheibe” which justifies using the letter S for disks.

[5] The geometric intersection number of two simple closed curves is the minimal number of intersections among all curves in general position that are isotopic to the given pair

$$\begin{tikzcd}
Z \arrow[r, "\hat{\phi}"] \arrow[d, "w"'] & Z' \arrow[d, "w'"] \\
D^2 \arrow[r, "\check{\phi}"] & D^2
\end{tikzcd}$$

with orientation preserving diffeomorphisms $\hat{\phi}$ and $\check{\phi}$ (see [B3] for more details). To obtain a simple wrinkled fibration from a surface diagram $\mathfrak{S} = (\Sigma; c_1, \dots, c_l)$ one constructs a 4–manifold $Z_{\mathfrak{S}}$ by attaching 2–handles to $\Sigma \times D^2$ along fiber framed push offs of the vanishing cycles $c_i \subset \Sigma \times \{\theta_i\}$ where $\theta_1, \dots, \theta_l \in S^1$ are ordered in counter. As shown in [B3] there is a natural way to define a simple wrinkled fibration $w_{\mathfrak{S}} \colon Z_{\mathfrak{S}} \to D^2$.

A surface diagram depicts a simple wrinkled fibration as seen from the higher genus perspective. Sometimes it is necessary to take a look from the lower genus side. For that purpose Williams introduced *surgered surface diagrams* [W2]. As the name suggests, they are the result of performing surgery on some vanishing cycle in a surface diagram. Instead of going for a formal definition we will just explain their structure.

Let $\mathfrak{S} = (\Sigma; c_1, \dots, c_l)$ be a surface diagram such that all vanishing cycles are in general position. We parametrize a neighborhood νc_1 by $S^1 \times (-1, 1)$ such that the non-empty intersections $c_i \cap \nu c_1$ correspond to lines of the form $\{\theta\} \times (-1, 1)$ and denote by Σ' the surface obtain by filling the two boundary components of $\Sigma \setminus \nu c_1$ with disks D_1 and D_2, ie the surgery on $c_1 \subset \Sigma$. We will refer to these disks as *surgery disks* in the following.

Since Σ can be reconstructed from Σ' once we know the two disks and an identification of their boundary, we can capture the whole surface diagram in Σ'. In order to do so we have to understand how the vanishing cycles appear in Σ'. Note that this way of picturing surfaces and curves therein is commonly used for Heegaard diagrams.

We denote by $c_i' = c_i \setminus \nu c_1$ the remains of c_i after the surgery. Clearly, if c_i is disjoint from c_1, then c_i' is a simple closed curve in Σ' which is disjoint from the surgery disks. However, if c_i intersects c_1, then c_i' is a collection of embedded arcs in Σ' whose endpoints lie on the boundaries of the surgery disks while the interiors are disjoint from the disks. Each surgery disk contains the same number of endpoints and the endpoints on the different disks are matched via the identification of the boundaries of the disks. Finally, the curve c_1 itself appears in Σ' as the boundary of either disk which we also denote by c_1'.

The collection $\mathfrak{S}' = (\Sigma'; c_1', \dots, c_l')$ is then a surgered surface diagram. Of course, we could have performed surgery on another vanishing cycle and the resulting diagram might look rather different. If necessary we will use the more precise notation $\mathfrak{S}'_{c_i}$ to indicate on which vanishing cycle we performed surgery, otherwise $\mathfrak{S}'$ will always stand for $\mathfrak{S}'_{c_1}$.

When we draw surgered surface diagrams the identification of the boundaries of the surgery disks is implicitly encoded as follows. Up to isotopy such an identification is determined by specifying one point on each boundary. To obtain such a pair of points we put an adjacent vanishing cycle of the one on which we performed surgery in minimal position so that it will appear as a single arc in the surgered diagram and we take its endpoints. Hence, as soon as we draw such an arc, we know how we have to identify the boundaries of the disks.

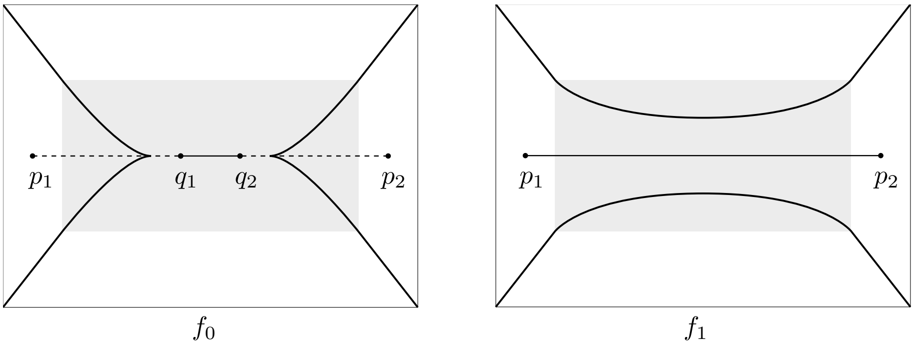

Figure 3. Critical images before and after a cusp merge. (The shaded regions shows the image of the support of the homotopy.)

3. Merge homotopies

Let $f_0\colon X \to B$ be a wrinkled fibration and assume that there are two cusps that point into the same component of $B \setminus \mathcal{C}_f$. It is well known that there is a homotopy f_s, $s \in [0,1]$ such that the critical image of f_1 looks as in Figure 3.[6] Since this type of homotopy merges two cusps, we will refer to it as a *cusp merge*. Cusp merge homotopies are the main tool for connecting different components of the critical loci of wrinkled fibrations, for example. (The inverse of a cusp merge will be called a *fold merge*.) Our main goal is to study the following problem.

Consider the reference points $p_i, q_i \in B$, $i = 1,2$, as shown in Figure 3 and let $\Sigma_i = f_0^{-1}(p_i)$ and $\Sigma_i' = f_0^{-1}(q_i)$. We can assume that the homotopy is supported in the preimage of the shaded region so that the fibers $f_s^{-1}(p_i)$ are independent of s and agree with Σ_i. It is easy to see that the surfaces Σ_1 and Σ_2 (resp. Σ_1' and Σ_2') are diffeomorphic. Indeed, parallel transport with respect to f_0 singles out an isotopy class of diffeomorphisms from Σ_1' to Σ_2'. In order to relate Σ_1 and Σ_2, however, we cannot use f_0; instead, we have to use the map f_1 that was obtained from a cusp merge homotopy. It turns out that the identification actually depends on the choice of the cusp merge homotopy and our main goal is to understand this dependence. As explained in the introduction, this is one of the central technical difficulties that one encounters when constructing or modifying simple wrinkled fibrations by homotopies.

For the statement of our result, recall that for a nonseparating simple closed curve $c \subset \Sigma$ in a closed, orientable surface there is a so called *surgery homomorphism* $\Phi_c\colon \mathrm{Mod}(\Sigma)(c) \to \mathrm{Mod}(\Sigma_c)$ where $\mathrm{Mod}(\Sigma)(c)$ consists of all mapping classes that fix the isotopy class of c and Σ_c is the surface obtained by surgery on c. We will say more about this in Section 3.2.

Theorem 3.1. *The set of identifications of* Σ_1 *and* Σ_2 *obtained from merging cusps is a torsor*[7] *for either of the groups*

$$\ker \Phi_{c_i} \cap \ker \Phi_{d_i} \subset \mathrm{Mod}(\Sigma_i), \quad i = 1,2$$

where $c_i, d_i \subset \Sigma_i$ *are the vanishing cycles of the cusps.*

There is an analogous problem for *fold merge* homotopies, the inverses of merging cusp merge, but it turns out that all possible fold merge homotopies give rise to

---

[6] This fact will also follow from our constructions below.

[7] ie it admits a free and transitive action of the group

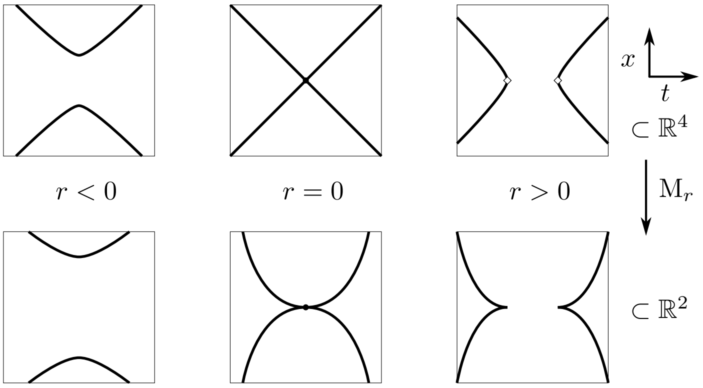

FIGURE 4. The critical locus and critical image of the merge homotopy.

isotopic identifications. We will return to this in Section 3.4. The majority of this section is devoted to the proof of Theorem 3.1 which will be finished in Section 3.3.

We begin by giving a precise definition of merge homotopies. Just as the fold and cusp singularities these can be described in terms of local models and the standard model is given by the map

$$\mathrm{M}_r(t,x,y,z) = \big(t,\ x^3 + 3(r-t^2)x + y^2 - z^2\big)$$

where $r \in [-1,1]$ is the time parameter. This family of maps describes a fold merge between M_{-1} and M_1 so that the inverse family M_{-r} yields a cusp merge in the other direction. Indeed, the critical locus of M_r is given by the equations $y = z = 0$ and $t^2 - x^2 = r$ and thus forms a hyperbola in the (t,x)-plane asymptotic to the diagonal and antidiagonal. For $r = 0$ the hyperbola is degenerate[8] while for $r \neq 0$ we have a parametrization

$$\mathcal{C}_{\mathrm{M}_r} = \big\{ \tfrac{1}{2}(\alpha + \tfrac{r}{\alpha}, \alpha - \tfrac{r}{\alpha}, 0, 0) \ \big|\ \alpha \in \mathbb{R} \setminus \{0\} \big\}$$

from which it is easy to deduce that the critical loci evolve with r as follows (see also Figure 4). For $r < 0$ we find only fold points and the branches of the hyperbolas lie in the sector containing the x–axis. As r approaches zero the hyperbolas degenerate meaning that the distance between the two branches, which is minimized by the two points $(0, \pm\sqrt{-r}, 0, 0)$, tends to zero. For $r = 0$ the degenerate hyperbola consisting of four fold arcs and a higher order singularity at the origin which we will refer to as the *merge point*. For $r > 0$ the hyperbolas become regular again and now lie in the sector containing the t–axis. The merge point dissolves into two cusps at $(\pm\sqrt{r}, 0, 0, 0)$, one on each branch.

The support of the homotopy M_r is all of $\mathbb{R}^4$ but for technical reasons it is more convenient to have models with compact support. Note that the interesting changes of the critical loci take place in the square $\{|t|, |x| \leq 2\}$. We thus choose a suitable cut off function $\kappa\colon \mathbb{R}^4 \to [0,1]$ which has constant value one in a large enough neighborhood of the origin containing the square $\{|t|, |x| \leq 2\}$ (see Remark 3.2 below) and define two homotopies with time parameter $s \in [0,1]$ by the formulas

$$\mathrm{CM}_s(t,x,y,z) := \mathrm{M}_{1-2\kappa(t,x,y,z)s}(t,x,y,z) \tag{3.1}$$

$$\mathrm{FM}_s(t,x,y,z) := \mathrm{M}_{2\kappa(t,x,y,z)s-1}(t,x,y,z). \tag{3.2}$$

These will serve as our standard models for cusp merge (CM) and fold merge (FM) homotopies. Outside the support of κ we find that CM_s agrees with its initial configuration $\mathrm{CM}_0 = \mathrm{M}_1$ and FM_s agrees with $\mathrm{FM}_0 = \mathrm{M}_{-1}$.

---

[8] ie the union of the diagonal and the antidiagonal

Remark 3.2. Here we explain the choice of κ. The confident reader may move on to Definition 3.3 right away. The point is that we have to make sure that the additional dependence on the variables caused by κ does not destroy the stability of the model for nonzero parameter values and does not change the qualitative structure of the critical loci. We focus on the cusp merge model, the arguments for the fold merge are almost verbatim. The critical locus of CM_s is described by the equations

$$t^2 - x^2 = -1 + 2(\kappa + x\tfrac{\partial\kappa}{\partial x})s, \quad y = -3sx\tfrac{\partial\kappa}{\partial y} \quad \text{and} \quad z = 3sx\tfrac{\partial\kappa}{\partial z}.$$

Note that in the regions where κ is constant these equations reduce to equations for $\mathrm{M}_{-1+2\kappa s}$

We choose a smooth function $\rho\colon \mathbb{R} \to [0,1]$ such that $\rho(u)$ is identically one for $|u| \leq r$ and identically zero for $u \geq R$ for some $R > r > 0$. We leave it to the reader to check the for any $\epsilon > 0$ one can find appropriate r, R and ρ with $r > R\epsilon$ and such that $|\rho'|$ and $|\rho''|$ are bounded by ϵ. We then define $\kappa(t,x,y,z) = \rho(t)\rho(x)\rho(y)\rho(z)$ and leave it to the interested reader to verify that this choice has the desired properties.

To give a flavor of the arguments we show how to deduce that critical points must satisfy $y = z = 0$. We first use the equation for y to estimate its absolute value as $|y| \leq R\epsilon < r$. From this we deduce that y is in the region where ρ is identically one which, in turn causes the right hand side of the equation, and thus y, to be zero. The same argument works for z and similar arguments show up in all remaining verifications.

Definition 3.3. A homotopy between wrinkled fibrations $f_s\colon X \to B$, $s \in [0,1]$, is called a *(cusp or fold) merge homotopy* if there are embeddings $\tilde{\mu}\colon \mathbb{R}^4 \to X$ and $\mu\colon \mathbb{R}^2 \to B$ such that f_s is supported on the image of $\tilde{\mu}$ and the diagram

$$\begin{tikzcd}
\mathbb{R}^4 \arrow[r, "\tilde{\mu}"] \arrow[d, "\mathrm{CM}_s \text{ or } \mathrm{FM}_s"'] & X \arrow[d, "f_s"] \\
\mathbb{R}^2 \arrow[r, "\mu"] & B
\end{tikzcd}$$

commutes for all $s \in [0,1]$.

Clearly, a cusp (resp. fold) merge homotopy is determined by an embedding of the initial configuration $\mathrm{CM}_0 = \mathrm{M}_1$ (resp. $\mathrm{FM}_0 = \mathrm{M}_{-1}$).

3.1. **Cusp merges via merge paths.**

We would like to pin down the geometric input needed to embed the initial cusp merge model

$$\mathrm{CM}_0(t,x,y,z) = \big(t, x^3 + 3(1-t^2)x + y^2 - z^2\big)$$

which for that purpose we divide into an *inner part* where $|t| \leq 1$ and *outer parts* where $|t| \geq 1 - \epsilon$ for some small $\epsilon > 0$.

We first observe that the outer parts can be matched with (a part of) the standard cusp model (2.1) in an orientation preserving manner. Since the two outer regions are exchanged by the diffeomorphism that sends (t,x,y,z) to $(-t,x,-y,z)$ it is enough to treat the region where $t \leq -1 + \epsilon$. A matching is constructed using the map $g(t) = 1 - t^2$ which provides a diffeomorphism of the interval $(-\infty, 0)$ onto $(-\infty, 1)$ and we obtain a commutative diagram:

$$\begin{tikzcd}
\{t \leq -(1-\epsilon)\} \times \mathbb{R}^3_{x,y,z} \arrow[r, "g\times\mathrm{id}"] \arrow[d, "\mathrm{CM}_0"'] & \{t \leq 2\epsilon - \epsilon^2\} \times \mathbb{R}^3_{x,y,z} \arrow[d, "\mathrm{C}"] \\
\{u \leq -(1-\epsilon)\} \times \mathbb{R}_v \arrow[r, "g\times\mathrm{id}"] & \{u \leq 2\epsilon - \epsilon^2\} \times \mathbb{R}_v
\end{tikzcd}$$

Consequently, an embedding of the outer parts of CM_0 is essentially equivalent to choosing model coordinates around the cusps that are supposed to be merged.

Next we focus on the inner part. There we find a distinguished horizontal path $\tilde\lambda_{\mathrm{st}} = \{(\tau,0,0,0)|\tau \in [-1,1]\}$ which is the straight line connecting the two cusps of CM_0 along which the cusps move toward the merge point as the homotopy flows; we denote its image by $\lambda_{\mathrm{st}} := \{(\tau,0)|\tau \in [-1,1]\}$. We will call $\tilde\lambda_{\mathrm{st}}$ and λ_{st} the *standard (cusp) merge path* and the *standard (cusp) merge arc*, respectively. Observe that the inner region agrees with $\tilde\lambda_{\mathrm{st}} \times \mathbb{R}^3$ so that we can consider it as a tubular neighborhood of $\tilde\lambda_{\mathrm{st}}$. We would like to obtain a parametrization of this neighborhood given by integrating certain vector fields in such a way that a splitting into vertical and horizontal parts becomes obvious.

We identify the normal bundle of $\tilde\lambda_{\mathrm{st}}$ with the Euclidean orthogonal complement of $T\tilde\lambda_{\mathrm{st}}$. The latter is spanned by ∂_t so that the former has a canonical framing given by ∂_x, ∂_y and ∂_z. In the interior of $\tilde\lambda_{\mathrm{st}}$ the normal bundle has a vertical part spanned by ∂_y and ∂_z and a vertical component given by the ∂_x–direction while at the endpoints all directions become vertical. However, ∂_x plays a special role since it spans the tangent space of the critical locus in the cusps. Also, it is intuitively clear that ∂_y and ∂_z are "more vertical" than ∂_x and we will thus only refer to ∂_y and ∂_z as the vertical framing of $\tilde\lambda_{\mathrm{st}}$.

We extend the framing along $\tilde\lambda_{\mathrm{st}}$ given by the vectors ∂_x, ∂_y and ∂_z to vector fields on $(-1,1) \times \mathbb{R}^3$ as follows. Note that CM_0 restricts to a (necessarily trivial) fiber bundle over $(-1,1) \times \mathbb{R}$ and it is easy to see that the map

$$\phi\big(t,x,y,z\big) = \big(t,\, x^3 + 3(1-t^2)x + y^2 - z^2\,, y, z\big)$$

provides a trivialization and the desired vector fields are:

$$\begin{aligned} X_0 &= d\phi^{-1}(\partial_x) = \tfrac{1}{3(x^2-t^2+1)}\partial_x \\ Y_0 &= d\phi^{-1}(\partial_y) = \partial_y - \tfrac{2y}{3(x^2-t^2+1)}\partial_x \\ Z_0 &= d\phi^{-1}(\partial_z) = \partial_z + \tfrac{2z}{3(x^2-t^2+1)}\partial_x \end{aligned} \tag{3.3}$$

Obviously, X_0 does not restrict to ∂_x on λ_{st} and is thus technically not an extension, but we do not lose anything by replacing ∂_x by X_0 in the first place. More or less by definition, X_0 is horizontal for CM_0 while Y_0 and Z_0 are vertical. Moreover, the vector fields commute such that we can integrate them simultaneously to obtain a parametrization of $\tilde\lambda_{\mathrm{st}} \times \mathbb{R}^3$. Note that, the trivial extensions of ∂_x, ∂_y, and ∂_z would also give a parametrization, but no splitting into horizontal and vertical components.

We now leave the local model and consider some wrinkled fibration $f\colon X \to B$. If we are given an embedding of CM_0, ie a commutative diagram

$$\begin{tikzcd} \mathbb{R}^4 \arrow[r, "\tilde\mu"] \arrow[d, "\mathrm{CM}_0"'] & X \arrow[d, "f"] \\ \mathbb{R}^2 \arrow[r, "\mu"] & B, \end{tikzcd}$$

then by the above remarks we obtain the following structures:

- an arc $\lambda := \mu(\lambda_{\mathrm{st}})$ in the base connecting two cusps through regular values,
- a horizontal lift $\tilde\lambda := \tilde\mu(\tilde\lambda_{\mathrm{st}})$ of λ to X which connects the cusps upstairs,
- a normal framing of $\tilde\lambda$ split into vertical and horizontal parts,
- extensions of the framing to horizontal and vertical vector fields in a neighborhood of $\tilde\lambda$ and

- a set of (partial) model coordinates around the cusps with which the above objects are compatible.

Remark 3.4. In the cusp model (2.1) there is a canonical line passing through the cusp, namely $\mathbb{R}\times\{0\}$. A similar discussion as for CM_0 shows that this line has a canonical lift $\mathbb{R}\times\{0\}^3$ together with a canonical framing. Via a set of model coordinates these lines map to line segments in the base and total space of a wrinkled fibration. The above mentioned compatibility with model coordinates means that λ and $\tilde\lambda$ should agree with the (framed) line segments near the cusps and the compatibility condition for the extensions of the framing is similar. In particular, λ is tangent to the cusp in the base.

All entries in our list make sense without the presence of an embedding of the cusp merge configuration and we will show that the data is actually enough to construct such an embedding. To set the stage for our result we introduce some terminology.

Definition 3.5. Let $f\colon X\to B$ be a wrinkled fibration. A *(cusp) merge arc* for f is an embedded arc in $\lambda\colon[-1,1]\to B$ connecting two cusps through regular values which is tangent to the cusps at its endpoints. A *(cusp) merge path* is a lift $\tilde\lambda\colon[-1,1]\to X$ of a merge arc λ in B connecting the cusps upstairs.

We will often simply speak of merge arcs and paths as exemplified by the last sentence in the above definition.

Remark 3.6. The concept of merge paths was also mentioned by Williams [W2] under the name “joining curves” in his discussion of the uniqueness of surface diagrams.

We have to discuss horizontal and vertical framings on cusp merge paths. Let f, λ and $\tilde\lambda$ be as above. Note that at the endpoints of $\tilde\lambda$ there is a distinguished 1–dimensional subspace of $T_{\tilde\lambda(\pm1)}X$ given by the tangent space of the critical locus $\mathcal{C}_f$, we will call this the *critical direction.*

We define a *horizontal framing* of $\tilde\lambda$ as a collection of nonzero, horizontal tangent vectors along $\tilde\lambda$ which nowhere tangent to $\tilde\lambda$ and point into the critical direction at endpoints. Since the horizontal part of the normal bundle of $\tilde\lambda$ is 1–dimensional, there are exactly two horizontal framings up to homotopy. Moreover, there is a unique choice whose push forward to B extends the velocity vector $\dot\lambda$ to an oriented basis.

Similarly, we define a vertical framing of $\tilde\lambda$ to be a collection of pairs of linearly independent vectors along $\tilde\lambda$ that are tangent to the fibers and are complementary to the critical direction at the endpoints. In other words, a vertical framing is a pair of lifts of $\tilde\lambda$ to the complement $\mathcal{V}_f^0$ of the zero section in $\mathcal{V}_f=\ker(df)$ which are point wise linearly independent and not critical at the endpoints. By a similar orientation argument as in the horizontal case it follows that a vertical framing is determined up to homotopy by a single such section.

For reason that will become clear very soon we also need a slightly different notion of vertical framing.

Definition 3.7. Let $f\colon X\to B$ be a wrinkled fibration and let $\tilde\lambda\colon[-1,1]\to X$ be a cusp merge path for f. A *projective vertical framing* (or *pv–framing*) of $\tilde\lambda$ is a lift $\widetilde{\boldsymbol{\lambda}}\colon[-1,1]\to\mathbb{P}(\mathcal{V}_f)$ such that $\widetilde{\boldsymbol{\lambda}}(\pm1)\neq T\mathcal{C}_f$. Here $\mathbb{P}(\mathcal{V}_f)$ is the fiber wise projectivization of $\mathcal{V}_f$.

Projective vertical framings are useful for our purposes since the cusp model admits an automorphism that changes the canonical vertical framing by a sign. To be precise, the canonical vertical framing at the origin of the cusp model is given by ∂_y and ∂_z and the (orientation preserving) diffeomorphism of $\mathbb{R}^4$ given by $(t,x,y,z) \mapsto (t,x,-y,-z)$ preserves the cusp model and has the described effect on the framing. In particular, if the cusp model is embedded in a wrinkled fibration then we can always change the induced vertical framing by a sign.

Remark 3.8. To summarize, a merge arc λ and a merge path $\tilde{\lambda}$ together with a pv-framing $\widetilde{\boldsymbol{\lambda}}$ covering λ fit into a commutative diagram of the form

$$\begin{tikzcd}
& \mathbb{P}(\mathcal{V}_f) \arrow[d, "\pi"] \\
& X \arrow[d, "f"] \\
{[-1,1]} \arrow[uur, "\widetilde{\boldsymbol{\lambda}}"] \arrow[ur, "\tilde{\lambda}"'] \arrow[r, "\lambda"] & B
\end{tikzcd}$$

where π is the natural projection. In the following, whenever one of these three curves is given, we will implicitly assume in our notation that the above diagram is completed, for example, if we are only given $\widetilde{\boldsymbol{\lambda}}$, then $\tilde{\lambda}$ and λ are defined according to the diagram.

Proposition 3.9. *Let $f \colon X \to B$ be a wrinkled fibration and let $\lambda \colon [-1,1] \to B$ be a cusp merge arc which is compatible with some model coordinates at its endpoints. If $\widetilde{\boldsymbol{\lambda}}$ is a pv–framed merge path covering λ which connects (the directions of) the vertical framings at the cusps induced by the coordinates, then there is a cusp merge homotopy starting at f whose pv–framed merge path agrees with $\widetilde{\boldsymbol{\lambda}}$.*

In the proof we will make use of the following construction which will also be important later on.

Lemma 3.10. *Let $f \colon X \to B$ be a wrinkled fibration together with a horizontal distribution $\mathcal{H}$ which is compatible with fixed model coordinates. If $\widetilde{\boldsymbol{\lambda}} \colon [-1,1] \to \mathbb{P}(\mathcal{V}_f)$ is a pv-framed merge path for some cusps of f compatible with the model coordinates, then there is a horizontal distribution $\mathcal{H}_0(\widetilde{\boldsymbol{\lambda}})$ such that*

(1) $\tilde{\lambda}$ is $\mathcal{H}_0(\widetilde{\boldsymbol{\lambda}})$–horizontal and
(2) $\mathcal{H}_0(\widetilde{\boldsymbol{\lambda}})$ agrees with $\mathcal{H}$ around the cusps and outside a neighborhood of $\tilde{\lambda}$.

Proof. Let $\lambda \colon [-1,1] \to B$ be the merge arc associated to $\widetilde{\boldsymbol{\lambda}}$. We first construct an extension of λ to an embedding $\nu\lambda \colon [-1,1] \times \mathbb{R} \to B$ as follows. Near the endpoints such an extension is provided by the model coordinates. For concreteness we focus on the cusp over $\lambda(-1)$. If the model coordinates are given by the diagram

$$\begin{tikzcd}
\mathbb{R}^4 \arrow[r, "\tilde{\kappa}"] \arrow[d, "\mathrm{C}"'] & X \arrow[d, "f"] \\
\mathbb{R}^2 \arrow[r, "\kappa"] & B,
\end{tikzcd}$$

then by compatibility there is some $\epsilon > 0$ such that for $t \in [-1,-1+\epsilon]$ we have $\lambda(t) = \kappa(t+1,0)$. On this interval we can thus define $\nu\lambda(t,s) = \kappa(t+1,s)$ and a similar argument provides an extension over $[1-\epsilon,1]$ using the other cusp. Over the remaining part of λ we choose an arbitrary extension that connects smoothly with the ones specified by the model coordinates. For simplicity we identify $\nu\lambda$ with its image in B and we also let $\mathring{\nu}\lambda = \nu\lambda\big((-1,1) \times \mathbb{R}\big)$.

Next, we trivialize f over $\mathring{\nu}\lambda$ to obtain a commutative diagram

$$\begin{tikzcd}
\Sigma' \times (-1,1) \times \mathbb{R} \arrow[r, "\Pi"] \arrow[d, "\mathrm{pr}"'] & f^{-1}(\mathring{\nu}\lambda) \arrow[d, "f"] \\
(-1,1) \times \mathbb{R} \arrow[r, "\nu\lambda"] & \mathring{\nu}\lambda
\end{tikzcd}$$

where $\Pi \colon \Sigma' \times (-1,1) \times \mathbb{R} \to f^{-1}(\mathring{\nu}\lambda)$ such that our horizontal distribution $\mathcal{H}$ agrees with $\Pi_* \langle \partial_u, \partial_v \rangle$ where (u,v) are coordinates on $(-1,1) \times \mathbb{R}$. In such a trivialization $\mathbb{P}(\mathcal{V}_f)$ corresponds to $\mathbb{P}(T\Sigma') \times (-1,1) \times \mathbb{R}$ and thus $\widetilde{\boldsymbol{\lambda}}$ corresponds to a curve $\boldsymbol{\lambda} \colon [-1,1] \to \mathbb{P}(T\Sigma')$ in the sense that $\widetilde{\boldsymbol{\lambda}}(t) = \Pi\big(\boldsymbol{\lambda}(t), t, 0\big)$. Moreover, by the compatibility with the model coordinates $\boldsymbol{\lambda}$ is constant near its endpoints with values $L_\pm \in T_{p_\pm}\Sigma'$.

An extension of the usual point pushing construction provides a diffeomorphism

$$\operatorname{push}(\boldsymbol{\lambda}) \colon (\Sigma', L_-) \longrightarrow (\Sigma', L_+). \tag{3.4}$$

which is realized by an isotopy $(\phi_s^{\boldsymbol{\lambda}})_{s \in (-1,1)}$ of Σ', also constant near ± 1, in the sense that $\operatorname{push}(\boldsymbol{\lambda}) = \phi_1^{\boldsymbol{\lambda}}$ where the right hand side is the obvious constant extension of the isotopy for $s = 1$.

For $x \in \Sigma'$ we denote by $\dot{\phi}_\tau^{\boldsymbol{\lambda}}(x)$ the tangent vector of the curve $\phi_s^{\boldsymbol{\lambda}}(x)$ at $s = \tau$ and define a new horizontal distribution on $f^{-1}(\mathring{\nu}\lambda)$ by

$$\mathcal{H}_0(\boldsymbol{\lambda})|_{\Pi(x,u,v)} = \Pi_* \Big\langle \partial_u|_{(x,u,v)} + \rho(v)\dot{\phi}_u^{\boldsymbol{\lambda}}\big((\phi_u^{\boldsymbol{\lambda}})^{-1}(x)\big), \partial_v|_{(x,u,v)} \Big\rangle$$

where $\rho \colon \mathbb{R} \to \mathbb{R}$ is a function with compact support which has constant value one in a neighborhood of zero. By construction $\mathcal{H}_0(\boldsymbol{\lambda})$ agrees with $\mathcal{H}$ over the ends of $\mathring{\nu}\lambda$ and thus can be extended by $\mathcal{H}$ across the rest of X. Moreover, the fact that $\tilde{\lambda}(t) = \Pi\big(\phi_t^{\boldsymbol{\lambda}}(p_+), t, 0\big)$ readily implies that $\tilde{\lambda}$ is $\mathcal{H}_0(\boldsymbol{\lambda})$–horizontal. ☐

Proof of Proposition 3.9. For convenience, let $\mathcal{H}$ be a horizontal distribution for f that is compatible with the chosen model coordinates and let $\mathcal{H}_0(\widetilde{\boldsymbol{\lambda}})$ be the horizontal distribution constructed from $\mathcal{H}$ in Lemma 3.10.

As explained above, the model coordinates provide an embedding of the outer parts of the cusp merge configuration. To embed the inner part we first lift the pv-framing on $\tilde{\lambda}$ to an honest vertical framing which agrees with the canonical framing over $\lambda(-1)$ and, possibly up to a sign, with the one over $\lambda(1)$. If the sign is nontrivial we adjust the canonical framing by changing the model coordinates on that side by sending (t,x,y,z) to $(t,x,-y,-z)$. Moreover, we choose an arbitrary horizontal framing with values in $\mathcal{H}_0(\widetilde{\boldsymbol{\lambda}})$.

The model coordinates provide extensions of the framings to commuting vector fields near the cusps which we can further extend to a neighborhood of $\tilde{\lambda}$. These vector fields play the role of X_0, Y_0 and Z_0 on page 12 and, as explained there, by integrating them we obtain an embedding of the inner part of the merge model such that the pv-framed merge path is given by $\widetilde{\boldsymbol{\lambda}}$. ☐

The above results indicate that the ambiguity for embedding a cusp merge is controlled by the group $\pi_1(\mathbb{P}(T\Sigma'), L_-)$. Our next goal is to relate this group to the mapping class group of a fiber on the other side of the cusp.

3.2. **A brief digression on mapping class groups.**

Let Σ be a compact, connected, orientable surface and let $\mathrm{Diff}^{(+)}(\Sigma)$ be the group of (orientation preserving) diffeomorphisms of Σ where the product is given by composition. We will need some slightly non-standard mapping class group terminology that we shall review presently.

Any diffeomorphism $T \in \mathrm{Diff}(\Sigma)$ gives rise to a diffeomorphism of the tangent bundle $T\Sigma$ via its derivative $dT\colon T\Sigma \to T\Sigma$. Moreover, the action of dT on (the image of) the zero section can be identified with the action of T on Σ. We henceforth consider Σ as embedded in $T\Sigma$ via the zero section.

Given a collection of subsets $P, S_1, \dots, S_m \subset T\Sigma$ we define $\mathrm{Diff}_P^{(+)}(\Sigma; S_1, \dots, S_m)$ as the subgroup of $\mathrm{Diff}^{(+)}(\Sigma)$ of all diffeomorphisms that fix P point wise and each S_i set wise and we let

$$\mathrm{Mod}_P(\Sigma; S_1, \dots, S_m) = \pi_0\left(\mathrm{Diff}_P^{+}(\Sigma; S_1, \dots, S_m)\right).$$

Given further subsets $A_1, \dots, A_n \subset T\Sigma$ we define

$$\mathrm{Mod}_P(\Sigma; S_1, \dots, S_m)(A_1, \dots, A_n) \subset \mathrm{Mod}_P(\Sigma; S_1, \dots, S_m)$$

to be the subgroup of all mapping classes that have representative in the subgroup $\mathrm{Diff}_P^{(+)}(\Sigma; S_1, \dots, S_m, A_1, \dots, A_n) \subset \mathrm{Diff}_P^{(+)}(\Sigma; S_1, \dots, S_m)$.

In the present paper, we will always assume that $P = \partial\Sigma$. For that reason we will drop the subscript P from our notation. (We gave the general definition in order to be consistent with other work of the second named author.) Moreover, in our context the S_i will be finite sets of tangent vectors or tangent lines while the A_j will be simple closed curves in Σ. Note that for zero vectors we recover the more common notion of marked points. In the case of a single tangent line we obtain the following generalization of the Birman exact sequence for the generalized point pushing construction encountered in the proof of Lemma 3.10.[9]

Lemma 3.11. *Let Σ' be a compact, orientable surface and let $L \in \mathbb{P}(T_p\Sigma')$ with p contained in the interior of Σ'. There is an exact sequence*

$$\cdots \to \pi_1(\mathrm{Diff}^+(\Sigma'), \mathrm{id}) \to \pi_1(\mathbb{P}(T\Sigma'), L) \xrightarrow{\text{push}} \mathrm{Mod}(\Sigma'; L) \xrightarrow{F_L} \mathrm{Mod}(\Sigma') \to 1$$

which reduces to a short exact sequence if $\chi(\Sigma) < 0$.

Proof. This is an easy adaption of the proof of the classical Birman exact sequence. We consider the map $\mathrm{ev}_L\colon \mathrm{Diff}^+(\Sigma) \to \mathbb{P}(T\Sigma)$ defined by $\mathrm{ev}_L(\phi) = d\phi(L)$. The arguments in [FM, Chapter 4.2.3] can be modified to show that ev_L is a fiber bundle with fiber $\mathrm{Diff}^+(\Sigma; L)$. The desired exact sequence then follows from the long exact sequence of homotopy groups and the short exactness follows from the contractibility of the (components of) the diffeomorphism groups of hyperbolic surfaces. □

Next, let Σ be a closed surface of genus g and let $c, d \subset \Sigma$ be two simple closed curves that intersect transversely in a single point (such as the vanishing cycles next to a cusp in a wrinkled fibration). We choose tubular neighborhoods νc and νd such that the closure of $\nu(c \cup d) = \nu c \cup \nu d$, denoted by $\bar{\nu}(c \cup d)$, is a one-holed torus with smooth boundary in Σ. We denote by Σ_c, Σ_d and $\Sigma_{c,d}$ the surfaces obtain by surgery on c or d, resp. symmetric surgery on c and d. Note that all these surfaces are obtained by gluing a disk to $\Sigma^\circ = \Sigma \setminus \nu(c \cup d)$ so that they are all diffeomorphic.

We first focus on $\Sigma_{c,d}$ and denote by D the disk glued to Σ° to obtain $\Sigma_{c,d}$.

Lemma 3.12. *Given a tangent line $L \in \mathbb{P}(T_p\Sigma_{c,d})$ over a point $p \in \mathring{D}$ there is a canonical isomorphism*

$$\Psi_L\colon \mathrm{Mod}(\Sigma_{c,d}; L) \xrightarrow{\cong} \mathrm{Mod}(\Sigma)(c, d).$$

Proof. It is easy to see that the groups $\mathrm{Mod}(\bar{\nu}(c \cup d))(c, d)$ and $\mathrm{Mod}(D; L)$ are infinite cyclic; the former group is generated by the Δ–twist $\Delta_{c,d} = (t_c t_d)^3$ while the latter is generated by a right-handed half twist h_p around $p \in D$. Note that both, $\Delta_{c,d}$ and h_p, square to a right handed Dehn twist about the boundary curve of the respective surface. We thus obtain a natural isomorphism

---

[9] This is probably well known but we were unable to find a precise reference.

$$\mathrm{Mod}(D;L) \xrightarrow{\cong} \mathrm{Mod}(\bar{\nu}(c \cup d))(c,d)$$

by sending h_p to $\Delta_{c,d}$ and to obtain Ψ_L we simply invoke the short exact sequences

$$1 \to \big\langle (t_{\partial\Sigma^\circ}^{-1}, h_p^2) \big\rangle \to \mathrm{Mod}(\Sigma^\circ) \times \mathrm{Mod}(D;L) \to \mathrm{Mod}(\Sigma_{c,d};L) \to 1$$

and

$$1 \to \big\langle (t_{\partial\Sigma^\circ}^{-1}, \Delta_{c,d}^2) \big\rangle \to \mathrm{Mod}(\Sigma^\circ) \times \mathrm{Mod}(\bar{\nu}(c \cup d))(c,d) \to \mathrm{Mod}(\Sigma)(c,d) \to 1.$$

□

We thus obtain a homomorphism from $\pi_1(\mathbb{P}(T\Sigma_{c,d}),L)$ into $\mathrm{Mod}(\Sigma)$ defined as the composition

$$\pi_1(\mathbb{P}(T\Sigma_{c,d}),L) \xrightarrow{\text{push}} \mathrm{Mod}(\Sigma_{c,d};L) \xrightarrow{\Psi_L} \mathrm{Mod}(\Sigma)(c,d) \hookrightarrow \mathrm{Mod}(\Sigma). \tag{3.5}$$

whose kernel is described in Lemma 3.11. Our next task is to determine its image. For that purpose we recall the definition of the *surgery homomorphism*

$$\Phi_c \colon \mathrm{Mod}(\Sigma)(c) \longrightarrow \mathrm{Mod}(\Sigma_c)$$

which is obtained by choosing a diffeomorphism that fixes c set wise, identifying the complement $\Sigma \setminus c$ with Σ_c with one marked point on each surgery disk and then forgetting the marked points. These homomorphisms and their kernel were introduced in the context of broken Lefschetz fibrations by Baykur [B2] and were further studied in the context of (simple) wrinkled fibrations by the authors [H2,B3].

Proposition 3.13. *The image of* (3.5) *agrees with* $\ker \Phi_c \cap \ker \Phi_d$. *It is isomorphic to its source* $\pi_1(\mathbb{P}(T\Sigma_{c,d}),L)$ *for* $g \geq 3$ *while, in the low genus cases, it is generated by* $\Delta_{c,d} = (t_c t_d)^3$ *which has infinite order for* $g = 2$ *and order two for* $g = 1$.

Proof. As mentioned above, the three surfaces Σ_c, Σ_d and $\Sigma_{c,d}$ are all obtained from $\Sigma^\circ = \Sigma \setminus \nu(c \cup d)$ by filling the boundary with a disk. From this we see that, up to isotopy relative to Σ°, there are unique diffeomorphisms between any two of the surfaces. In particular, their mapping class groups are canonically isomorphic. With these canonical isomorphisms we obtain a diagram

$$\begin{tikzcd}
\mathrm{Mod}(\Sigma)(c) \arrow[rr, "\Phi_c"] & & \mathrm{Mod}(\Sigma_c) \arrow[d, "\cong"] \\
\mathrm{Mod}(\Sigma)(c,d) \arrow[u, "\mathrm{incl}"] \arrow[d, "\mathrm{incl}"'] & \mathrm{Mod}(\Sigma_{c,d};L) \arrow[l, "\Psi_L", "\cong"'] \arrow[r, "F_L"] & \mathrm{Mod}(\Sigma_{c,d}) \\
\mathrm{Mod}(\Sigma)(d) \arrow[rr, "\Phi_d"] & & \mathrm{Mod}(\Sigma_d) \arrow[u, "\cong"']
\end{tikzcd}$$

whose commutativity can be checked by carefully going through the definitions. It follows that Ψ_L^{-1} maps $\ker \Phi_c \cap \ker \Phi_d$ isomorphically onto $\ker F_L$ and Lemma 3.11 identifies this group with the image of $\pi_1(\mathbb{P}(T\Sigma_{c,d}),L)$ under the pushing map. This proves the first statement and the second is an easy consequence of Lemma 3.11. □

3.3. **Parallel transport before and after merging cusps.** We are finally in a position prove Theorem 3.1. To set up the notation let $f\colon X \to B$ be a wrinkled fibration together with a horizontal distribution $\mathcal{H}$. We fix model coordinates around the cusps with which we assume all merge arcs and paths to be compatible. Let $\lambda\colon [-1,1] \to B$ be a cusp merge arc for f and let $\Lambda\colon [-1-\epsilon, 1+\epsilon] \to B$ be a small extension of λ whose ends run into the part of the higher genus region which is covered by the model coordinates. As reference points we choose $\{p_1, p_2\} = \{\lambda(\pm(1+\epsilon))\}$ and $\{q_1, q_2\} = \{\lambda(\pm(1-\epsilon))\}$ and, as before, we denote the fibers by $\Sigma_i = f^{-1}(p_i)$ and $\Sigma_i' = f^{-1}(q_i)$. Recall that the model coordinates give rise to tangent lines $L_i \in \mathbb{P}(T\Sigma_i')$.

Given a pv-framed merge path $\widetilde{\boldsymbol{\lambda}}$ covering λ we denote by $f_t(\widetilde{\boldsymbol{\lambda}})$ the cusp merge homotopy constructed in Proposition 3.9. Note that we obtain a family of horizontal distributions $\mathcal{H}_t(\widetilde{\boldsymbol{\lambda}})$ by modifying $\mathcal{H}_0(\widetilde{\boldsymbol{\lambda}})$ according to the cusp merge model. To shorten the notation we denote by $\varphi(\widetilde{\boldsymbol{\lambda}})$ (resp. $\varphi'(\widetilde{\boldsymbol{\lambda}})$) the isotopy class of the parallel transport $\mathrm{PT}_{\Lambda}^{\mathcal{H}_1(\widetilde{\boldsymbol{\lambda}})}\colon \Sigma_1 \to \Sigma_2$ (resp. $\mathrm{PT}_{\lambda}^{\mathcal{H}_0(\widetilde{\boldsymbol{\lambda}})}\colon \Sigma_1' \to \Sigma_2'$).

We first study the parallel transport before performing the homotopy.

Lemma 3.14. *Let $\widetilde{\boldsymbol{\lambda}}_1$ and $\widetilde{\boldsymbol{\lambda}}_2$ be two pv-framed merge paths covering λ. Then the concatenation $\widetilde{\boldsymbol{\lambda}}_1\widetilde{\boldsymbol{\lambda}}_2^{-1}$ gives rise to an element of $\pi_1(\mathbb{P}(T\Sigma_1), L_1)$, also denoted by $\widetilde{\boldsymbol{\lambda}}_1\widetilde{\boldsymbol{\lambda}}_2^{-1}$, and we have $\varphi'(\widetilde{\boldsymbol{\lambda}}_2)^{-1}\varphi'(\widetilde{\boldsymbol{\lambda}}_1) = \mathrm{push}(\widetilde{\boldsymbol{\lambda}}_1\widetilde{\boldsymbol{\lambda}}_2^{-1}) \in \mathrm{Mod}(\Sigma_1; L_1)$.*

Proof. By parallel transporting $\widetilde{\boldsymbol{\lambda}}_1\widetilde{\boldsymbol{\lambda}}_2^{-1}$ back to Σ_1' along λ with respect to some horizontal distribution at each time we obtain a loop in $\mathbb{P}(T\Sigma_1')$ based at L_1 and it is easy to see that different horizontal distributions give rise to homotopic loops. The verification of the second claim is not necessarily pleasant but ultimately straightforward from the construction of $\mathcal{H}_0(\widetilde{\boldsymbol{\lambda}})$. □

Next, let $c_i, d_i \subset \Sigma_i$ be the vanishing cycles induces by the cusps at $\lambda(\pm 1)$. Note that, since Σ_1 maps to the region covered by the model coordinates, the vanishing cycles intersect transversely in one point and we obtain an isomorphism

$$\Psi_{L_1}\colon \mathrm{Mod}(\Sigma_1'; L_1) \to \mathrm{Mod}(\Sigma_1)(c_1, d_1)$$

as in the previous section by identifying Σ_1' with the symmetric surgery on c_1 and d_1 using the parallel transport along Λ.

Lemma 3.15. *The isomorphism Ψ_{L_1} maps $\varphi'(\widetilde{\boldsymbol{\lambda}}_2)^{-1}\varphi'(\widetilde{\boldsymbol{\lambda}}_1)$ to $\varphi(\widetilde{\boldsymbol{\lambda}}_2)^{-1}\varphi(\widetilde{\boldsymbol{\lambda}}_1)$.*

Proof. Let $U_i \subset X$ denote the images of our fixed model coordinates. Then the intersection $\Sigma_i' \cap U_i$ is an open disks D_i while $\Sigma_i \cap U_i$ is a one-holed torus T_i. By parallel transport with respect to $\mathcal{H}$ we obtain identifications between $\Sigma_i \setminus T_i$ and $\Sigma_i' \setminus D_i$. (Note that $\mathcal{H}_0(\widetilde{\boldsymbol{\lambda}}_i)$ can be constructed to agree with $\mathcal{H}$ over the relevant part of Λ so that we could also use $\mathcal{H}_0(\widetilde{\boldsymbol{\lambda}}_i)$.)

One can show that in the cusp merge model CM_s the parallel transport along the t–axis from $\mathrm{CM}_s^{-1}(-t,0)$ to $\mathrm{CM}_s^{-1}(t,0)$ is given by $(-t,x,y,z) \mapsto (t,x,y,z)$ given that $(\pm t, 0)$ are regular values and that the points are not contained in the vanishing set. Since the model coordinates are matched with the outer parts of the merge model, we can deduce that $\varphi'(\widetilde{\boldsymbol{\lambda}}_2)^{-1}\varphi'(\widetilde{\boldsymbol{\lambda}}_1)$ (resp. $\varphi(\widetilde{\boldsymbol{\lambda}}_2)^{-1}\varphi(\widetilde{\boldsymbol{\lambda}}_1)$) maps D_1 (resp. T_1) to itself by either the identity or a rotation by 180 degrees (resp. a hyperelliptic involution) depending on whether $\widetilde{\boldsymbol{\lambda}}_1\widetilde{\boldsymbol{\lambda}}_2^{-1} \in \pi_1(\mathbb{P}(T\Sigma_1), L)$ lifts to a loop in $T\Sigma_1$.

A comparison with the definition of Ψ_{L_i} then finishes the proof. □

Proof of Theorem 3.1. Given two cusp merge homotopies, it is easy to see that the difference of parallel transports must be contained in the group $\ker \Phi_{c_i} \cap \ker \Phi_{d_i}$. On the other hand, it follows from Proposition 3.9 together with Lemmas 3.14 and 3.15 and Proposition 3.13 that any element can be realized. □

3.4. **The case of fold merges.** After our extensive study of cusp merges we now take a look at fold merges. Let $f\colon X \to B$ be a wrinkled fibration and assume that a square in B intersects the critical image in two parallel fold arcs. We choose a horizontal distribution $\mathcal{H}$ for f, a reference point in the middle region of the square and one reference arc as in Example 2.7 for each fold arc, say γ_c and γ_d. In order to perform a fold merge it is necessary and sufficient that the vanishing sets in the reference fiber Σ are two simple closed curves $c, d \subset \Sigma$ with geometric intersection number one. We will call this structure a *fold merge configuration* and refer to Σ as the *inner fiber*.

A look at the local model looks that, if $\mathcal{H}$ is compatible with an embedding of the initial fold merge configuration FM_0, then the vanishing cycles $c, d \subset \Sigma$ intersect transversely in one point. On the other hand, given a horizontal distribution whose vanishing cycles exhibit this behavior, one can construct a compatible embedding of FM_0 and it is easy to see that one can always find such a horizontal distribution.

We will thus assume that our distribution $\mathcal{H}$ has this property. In this situation, it is convenient to label the *outer fibers*, that is, the fibers over the other endpoints of γ_c and γ_d, by Σ_c and Σ_d, respectively, since the parallel transport provides an identification with the surgered surfaces. We choose a regular neighborhood $\nu(c \cup d) = \nu c \cup \nu d$ as in the discussion before Lemma 3.12. The parallel transport along γ_c then maps $\nu(c \cup d) \setminus c$ onto a twice punctured disk $D_c \subset \Sigma_c$ in which d appears as an arc d' connecting the two punctures which we can think of as marked points. The analogous statement holds with the roles of c and d interchanged. The crucial observation is that parallel transport yields a diffeomorphism

$$(\mathrm{PT}^{\mathcal{H}}_{\gamma_c})^{-1} \circ \mathrm{PT}^{\mathcal{H}}_{\gamma_d} \colon \Sigma_c \setminus D_c \longrightarrow \Sigma_d \setminus D_d$$

between the complements of these disks and, as mentioned before, up to isotopy there is a unique extension to a diffeomorphism $\Sigma_c \to \Sigma_d$. Moreover, one can show that the parallel transport *after* performing a fold merge will be in this isotopy class. So up to isotopy, there is a unique identification of the outer fibers that can be obtained after merging folds which can already be described *before* actually merging folds.

4. Homotopy moves for surface diagrams

In this section, we discuss the relation between several types of homotopies which appear in [W2] and the corresponding modifications of surface diagrams.

4.1. **Multislides.** We first consider multislide deformations. As explained in [W2], a multislide deformation is a fold merge followed by a cusp merge, and the support of this homotopy is contained in a neighborhood of a pair of fold arcs. In particular, the argument in Subsection 3.3 implies the following proposition.

Proposition 4.1. *Let $w : X \to D^2$ be a simple wrinkled fibration with surface diagram $\mathfrak{S} = (\Sigma; c_1, \dots, c_l)$ and assume that there exists some $1 < k < l$ such that c_1 and c_k intersect in one point.*

(i) If $w' : X \to D^2$ is obtained from w by applying a multislide deformation around the two fold arcs whose vanishing cycles are c_1 and c_k, respectively. Then there exists an element $\phi \in \ker(\Phi_{c_1}) \cap \ker(\Phi_{c_k})$ such that the surface diagram of w' is given by

$$\big(\Sigma; c_1, \dots, c_k, \phi(c_{k+1}), \dots, \phi(c_l)\big). \tag{4.1}$$

(ii) *For any* $\phi \in \ker(\Phi_{c_1}) \cap \ker(\Phi_{c_k})$*, there exists a merge deformation from* w *to a simple wrinkled fibration whose surface diagram is given by* (4.1).

4.2. **Shifts and generalized shifts.** As is described in [W2], a shift deformation also consists of a fold merge and a cusp merge. However, this homotopy is different from a multislide deformation in the following sense: one of cusp points to which a cusp merge is applied in a shift deformation is neither of the cusp points which appear in the initial fold merge (cf. Figure 5). Moreover, this kind of deformation is determined up to homotopy once we give a merge path and its framing for a cusp merge after applying the initial fold merge. As explained in [W2], there is a canonical way to take such a merge path. A deformation determined by this merge path is called a shift deformation. In this article, we call any deformations which change a base diagram as described in Figure 5 a *generalized shift deformation.*

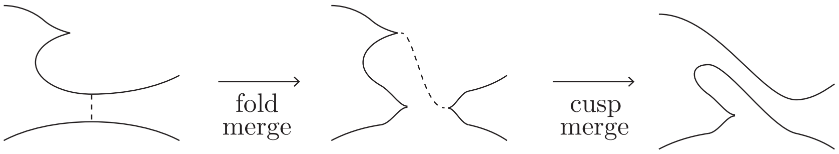

Figure 5. The base diagrams in a generalized shift deformation. The fold and cusp merges are applied along the dashed arcs.

Proposition 4.2. *Let* $w : X \to D^2$ *be a simple wrinkled fibration with surface diagram* $\mathfrak{S} = (\Sigma; c_1, \dots, c_l)$ *and assume that there exists some* $1 < k < l$ *such that* c_k *and* c_l *intersect in one point.*

(i) *If* $w' : X \to D^2$ *is obtained from* w *by a generalized shift deformation whose initial fold merge is applied around the two fold arcs with vanishing cycles* c_k *and* c_l*. Then the surface diagram of* w' *is given by*

$$\big(\Sigma; c_1, \dots, c_k, c_l, \chi(c_{k+1}), \dots, \chi(c_{l-1})\big) \tag{4.2}$$

where $\chi \in \mathrm{Mod}(\Sigma)$ *satisfies the following properties;*

(a) $\chi t_{c_l}^{-1} t_{c_k}^{-1} \in \ker(\Phi_{c_l})$*,*

(b) $\chi t_{c_1}^{-1} t_{c_l}^{-1} \in \ker(\Phi_{c_1})$*.*

(ii) *For any* $\chi \in \mathrm{Mod}(\Sigma)$ *satisfying the conditions (a) and (b) above, there exists a generalized shift deformation from* w *to a simple wrinkled fibration whose surface diagram is given by* (4.2).

Proof. Figure 6 describes the image of a neighborhood of the fold arcs with the vanishing cycles c_1, c_k and c_l. We take the points p_0, p_1, $q_0, \tilde{q}_0, q_1$, $r_0, \tilde{r}_0, r_1 \in S^2$ and the oriented paths γ_0, γ_1, $\delta_1, \delta_2, \delta_3$, $\varepsilon_1, \varepsilon_2, \varepsilon_3 \subset S^2$ as described in Figure 6.

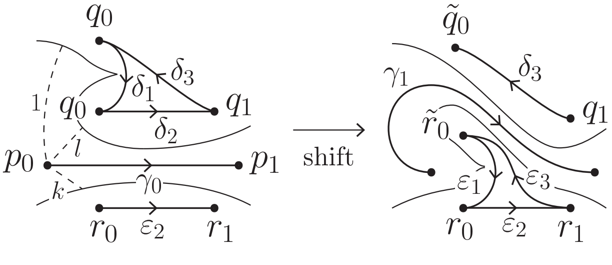

Figure 6. The dashed curves describe reference paths which give vanishing cycles c_1, c_k and c_l.

The path γ_i, together with a horizontal distribution $\mathcal{H}$ of w, gives a parallel transport $\varphi_i = PT_{\gamma_i}^{\mathcal{H}} : w^{-1}(p_0) \to w^{-1}(p_1)$ $(i = 0, 1)$. We denote by χ the isotopy class of the diffeomorphism $\varphi_1^{-1} \circ \varphi_0 : \Sigma \to \Sigma$ (note that the reference fiber $w^{-1}(p_0)$ is identified with Σ). A surface diagram derived from w' is equal to the following sequence:

$$\big(\Sigma; c_1, \ldots, c_k, c_l, \chi(c_{k+1}), \ldots, \chi(c_{l-1})\big)$$

Thus, we can prove the statement (i) of Proposition 4.2 once we prove that the element χ defined as above satisfies the conditions (a) and (b) in Proposition 4.2. It is easy to see that the image $\Phi_{c_l}(\chi t_{c_l}^{-1} t_{c_k}^{-1} t_{c_l})$ is a monodromy along the loop obtained by connecting $\varepsilon_1, \varepsilon_2$ and ε_3. Since this loop is nullhomotopic, the element $\chi t_{c_l}^{-1} t_{c_k}^{-1} t_{c_l}$ is contained in the kernel of Φ_{c_l}. This implies $\chi t_{c_l}^{-1} t_{c_k}^{-1}$ is also contained in $\ker \Phi_{c_l}$. It is also easy to prove that the image $\Phi_{c_1}(\chi t_{c_1}^{-1} t_{c_l}^{-1} t_{c_1})$ is a monodromy along the loop obtained by connecting δ_1, δ_2 and δ_3. In particular, this image is trivial and this proves that $\chi t_{c_1}^{-1} t_{c_l}^{-1}$ is contained in $\ker \Phi_{c_1}$.

We next prove the statement (ii) of Proposition 4.2. Let $\chi' \in \mathrm{Mod}(\Sigma)$ be an element satisfying the conditions (a) and (b). The element $\chi \chi'^{-1}$ is contained in the group $\ker \Phi_{c_1} \cap \ker \Phi_{c_l}$. By Theorem 3.1, we can take a multislide deformation from the fibration w' such that the isotopy class of the diffeomorphism from $w'^{-1}(p_0)$ to $w'^{-1}(p_1)$ determined by γ_1 is equal to $[\varphi_1]\chi\chi'^{-1}$. A surface diagram obtained from the resulting fibration is the following sequence:

$$\big(\Sigma; c_1, \ldots, c_k, c_l, \chi'(c_{k+1}), \ldots, \chi'(c_{l-1})\big)$$

Since these successive homotopies can be regarded as a generalized shift deformation, this completes the proof of the statement (ii) of Proposition 4.2. ☐

There is a canonical way to take an element χ satisfying the conditions (a) and (b) in Proposition 4.2 up to multiplication of Delta twists. In the rest of this subsection, we will explain how to obtain this canonical one. Let $w : X \to D^2$ be a simple wrinkled fibration, and $(\Sigma; c_1, \ldots, c_l)$ be a surface diagram obtained from w. Assume that c_k intersects c_l in one point transversely. We denote by w' a fibration obtained by applying a fold merge to a pair of fold arcs with vanishing cycles c_k and c_l. As described in Figure 7, we take a base point p_0 in a lower-genus-fiber region of w', and a reference path γ from p_0. The path γ gives a surgered surface diagram which consists of two surgery disks D_1, D_2, and vanishing cycles or arcs in Σ_{c_l}. We can collapse the surgery disks to points and obtain the graph in Σ_{c_l} with two vertices. Denote the two points by $v_1, v_2 \in \Sigma_{c_l}$. The vanishing arcs corresponding to c_l and c_1 connect v_1 to v_2. In particular, we can obtain a loop η in $\Sigma_{c_l} \setminus \{v_2\}$ based at v_1 by connecting these edges and then missing the point v_2 by a small perturbation. It is easy to see that there is a unique element ξ_η in $\mathrm{Mod}(\Sigma)$ which satisfies the following conditions:

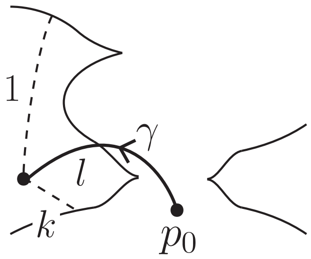

Figure 7. The base diagram of w'.

- ξ_η preserves the curve c_l, and maps the curve c_k to the curve c_1,
- ξ_η is a lift of the element $Push(\eta) \in \mathrm{Mod}(\Sigma_{c_l}; v_1, v_2)$ under the surgery homomorphism $\Phi_{c_l}^* : \mathrm{Mod}(\Sigma)(c_l) \to \mathrm{Mod}(\Sigma_{c_l}; v_1, v_2)$.

The element ξ_η is changed by multiplication of Δ_{c_k,c_l} when we change a perturbation in the construction of η. In particular, the element

$$\chi_{\mathrm{can.}} = \xi_\eta t_{c_k} t_{c_l} t_{c_k}$$

is uniquely determined from w' up to the multiplication of the Delta twists. It is easy to verify the following proposition, whose proof is left to the readers.

Proposition 4.3. *The element $\chi_{can.}$ satisfies the conditions (a) and (b) in Proposition 4.2.*

By Proposition 4.3, it is natural to expect the following conjecture holds.

Conjecture 4.4. *The element $\chi_{can.}$ gives a shift deformation.*

4.3. **Handleslides and stabilizations.** For the sake of completeness we list the effect of the two remaining basic homotopies of simple wrinkled fibrations on their surface diagrams: the *handleslide* and *stabilization* homotopies. The results were obtained by the second author in [H2]

The statement for handleslides is very similar to the one for multislides. However, we should care about the case when a genus of some component of a fiber in the middle bigon appeared in R_2-move is small.

Proposition 4.5. *Let $w\colon X \to D^2$ be a simple wrinkled fibration with surface diagram $\mathfrak{S} = (\Sigma; c_1, \dots, c_l)$ and assume that there exists some $1 < k < l$ such that c_1 and c_k are disjoint. We denote by Σ_{c_1,c_k} the surface obtained by applying surgeries along the curves c_1 and c_k.*

(i) If w' is obtained from w by a handleslide deformation, then for some element $\psi \in \ker(\Phi_{c_1}) \cap \ker(\Phi_{c_k})$, the surface diagram of w' is given by

$$\big(\Sigma; c_1, \dots, c_k, \psi(c_{k+1}), \dots, \psi(c_l)\big). \tag{4.3}$$

(ii) Suppose that every component of the surface Σ_{c_1,c_k} has a genus at least 2. Then, for any element $\psi \in \ker(\Phi_{c_1}) \cap \ker(\Phi_{c_k})$, there exists a handleslide deformation from w to a simple wrinkled fibration whose surface diagram is given by (4.3).

Remark 4.6. For the case that the surface Σ_{c_1,c_k} has a component with small genus, not every element in $\ker(\Phi_{c_1}) \cap \ker(\Phi_{c_k})$ can be realized by a handleslide deformation. For the detail about this case, see [H2].

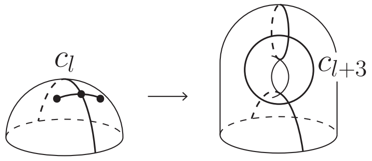

FIGURE 8. The procedure of obtaining the surface $\tilde{\Sigma}$ from Σ.

Proposition 4.7. *Let $w\colon X \to S^2$ be a simple wrinkled fibration. We denote by $\mathfrak{S} = (\Sigma; c_1, \dots, c_l)$ a surface diagram obtained by w.*

(i) If $w' : X \to S^2$ *is obtained from* w *by applying a stabilization deformation (that is, a flip and slip) to the fold arc with the vanishing cycle* c_l*. Then the surface diagram of* w' *is given by*

$$\big(\tilde{\Sigma}; c_1, \ldots, c_l, \tilde{\theta}(c_{l+3}), c_{l+2}, c_{l+3}, c_l\big), \tag{4.4}$$

where $\tilde{\Sigma}$ *is the surface obtained by replacing a disk neighborhood of a point on* c_l *by a once-punctured torus as described in Figure 8,* c_{l+2} *and* c_{l+3} *are the simple closed curves in* $\tilde{\Sigma}$ *as in Figure 8,* $\theta \in \mathrm{Mod}(\tilde{\Sigma})(c_l, c_{l+2})$ *is an element satisfying the following conditions:*
(a) $\Phi_{c_l}(\theta) = 1$*,*
(b) $\Phi_{c_{l+2}}(\theta) = t_{t_{c_{l-1}}(c_l)} \cdots t_{t_{c_1}(c_2)} t_{t_{c_l}(c_1)}$*,*
and we put $\tilde{\theta} = t_{t_{c_{l-1}}(c_l)} \cdots t_{t_{c_1}(c_2)} t_{t_{c_l}(c_1)} \theta^{-1}$*.*

(ii) Suppose that the genus of the fibration w *is at least* 3*. For any element* $\theta \in \mathrm{Mod}(\tilde{\Sigma})(c_l, c_{l+2})$ *satisfying the conditions (a) and (b), there exists a stabilization deformation from* w *to a simple wrinkled fibration whose surface diagram is given by* (4.4)*.*

For the statement for the lower genus cases we refer to [H2].

5. Applications

In this section we describe some constructions of simple wrinkled fibrations that involve cusp merge homotopies and show how to obtain surface diagrams. In order to do this we have to turn our theoretical understanding of parallel transport in cusp merge homotopy into a method which is useful in practice.

Let $f\colon X \to B$ be a wrinkled fibration that contains a cusp merge configuration as depicted in Figure 9 and fix a horizontal distribution $\mathcal{H}$. As indicated, we choose reference fibers Σ_i and Σ_i' near the cusps and another one Σ' further away in the lower genus region. We denote the vanishing cycles in Σ_i by c_i and d_i where the c_i correspond to the lower fold arcs.

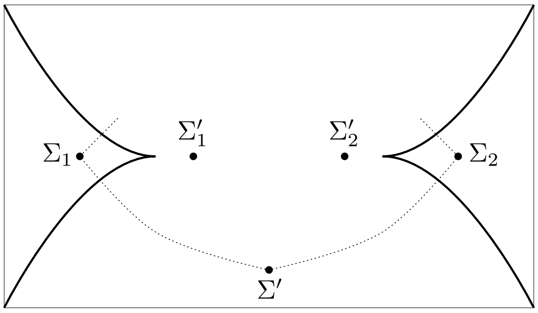

Figure 9. Matching surgered surface diagrams.

By parallel transport we can identify Σ' with the surgery on either $c_1 \subset \Sigma_1$ or $c_2 \subset \Sigma_2$ and each possibility gives rise to a pair of surgery disks $D_i^{\pm} \subset \Sigma'$ and an arc d_i' connecting the disks. Recall that with this data we can completely reconstruct the higher genus fiber Σ_i from Σ'. There is now an easy way to identify the higher genus fibers. We simply have to find a *matching isotopy* $\boldsymbol{\phi} = (\phi_t)$ of Σ' that moves the whole configuration $D_2^- \cup d_2' \cup D_2^+$ to $D_1^- \cup d_1' \cup D_1^+$. Clearly, such an isotopy induces a diffeomorphism $\tilde{\boldsymbol{\phi}}\colon \Sigma_2 \to \Sigma_1$.

To see that the identifications we obtain in this way are the same as the ones coming from cusp merges, we first observe that the choice of a matching isotopy is essentially equivalent to the choice of a path in $\mathbb{P}(T\Sigma')$. Indeed, it easy to see that from any path $\boldsymbol{\lambda}$ in $\mathbb{P}(T\Sigma')$ that connects a tangent spaces of d'_2 and d'_1 at interior points, we can construct a matching isotopy which realizes push$(\boldsymbol{\lambda})$. On the other hand, any matching isotopy gives rise to such a path as the trace of a tangent space to d'_2. For concreteness, let us fix tangent spaces $T_i \in \mathbb{P}(T\Sigma')$ of d'_i.

To make the connection to cusp merge homotopies, we denote the tangent lines in the lower genus fibers near the cusps by $L_i \in \mathbb{P}(\Sigma'_i)$. We can assume that, after trivializing the lower genus region using $\mathcal{H}$, the lines L_i correspond to the lines T_i. As a consequence, given any path in $\mathbb{P}(T\Sigma')$ from T_2 to T_1, we can construct a pv-framed merge path covering the obvious merge path and it is obvious that the parallel transport obtained after performing the corresponding cusp merge agrees with the identification obtain from the matching isotopy associated to $\boldsymbol{\lambda}$.

For examples of this procedure we refer to the upcoming Sections 5.1 and 5.2 where we construct surface diagram for Lefschetz fibrations as well as products of 3–manifolds with the circle.

5.1. Surface diagrams for Lefschetz fibrations.

It is easy to change a Lefschetz fibration into a simple wrinkled fibration by first wrinkling the Lefschetz singularities and then applying cusp merges. In this subsection we will explain how to obtain surface diagrams for the resulting simple wrinkled fibrations from (Lefschetz) vanishing cycle descriptions of the initial Lefschetz fibrations. As an example, we apply this procedure to the elliptic Lefschetz fibrations $f : E(n) \to S^2$.

We first recall how the Lefschetz and fold vanishing cycles behave in wrinkling homotopies. As explained in [L], a wrinkling homotopy changes a Lefschetz singularity into a circular singularity with three cusps and the corresponding fold vanishing cycles are related to the Lefschetz vanishing cycle as described in Figure 10.

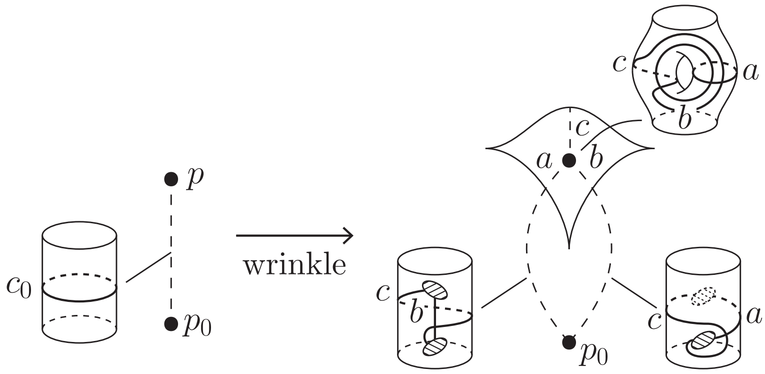

Figure 10. Surgered surface diagrams in a wrinkling homotopy.

We choose a Hurwitz system $\gamma_1, \ldots, \gamma_{6n}$ of the Lefschetz fibration $f : E(n) \to S^2$ such that the corresponding monodromy factorization is $(t_{d_1} \cdot t_{d_2})^{6n}$, where d_1, d_2 are simple closed curves in T^2 which generate the group $H_1(T^2)$ (these curves are described in the left side of Figure 11). As explained in the previous paragraph, a wrinkling homotopy changes vanishing cycles as described in Figure 11. We denote by $p_i \in S^2$ the images of Lefschetz singularity which is one of the end points of γ_i, and by $s_i \subset S^2$ the image of critical locus with three cusps derived from p_i (see the right side of Figure 11). We take simple closed curves c_1, c_2, c_3, c_4, c_5 in the genus-2

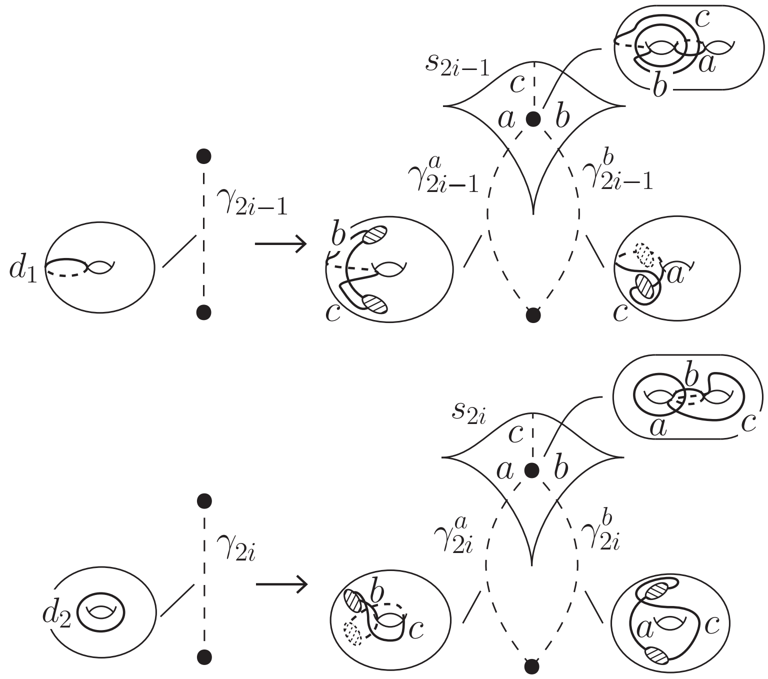

FIGURE 11. Wrinkling homotopies and the corresponding surgered surface diagrams.

surface Σ_2 as described in the left side of Figure 12. As we can see in the right side of Figure 11, a surface diagram of s_{2i-1} is described as follows:

$$\mathfrak{S}_{2i-1} = (\Sigma_2; a = c_3, b = c_2, c = t_{c_1}(c_2)),$$

while that derived from s_{2i} is described as follows:

$$\mathfrak{S}_{2i} = (\Sigma_2; a = c_2, b = c_3, c = t_{c_4}(c_3)).$$

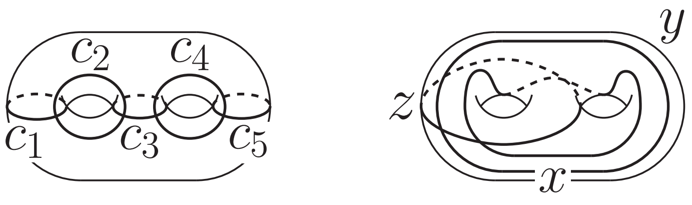

FIGURE 12. Simple closed curves in Σ_2.

To obtain a simple wrinkled fibration on $E(n)$ we first connect s_1 with s_2 by a cusp merge. We denote by $\widetilde{s}_{1,2}$ the resulting critical locus. The corresponding surgered surface diagram of $\widetilde{s}_{1,2}$ can be obtained by changing a surgered surface diagram derived from the reference path γ_1^a so that the surgery disks and the path c in this diagram match with those of the surgered surface diagram derived from γ_2^b. Since the surgery disks of these surgered surface diagrams coincide, this modification is equivalent to applying an element $\varphi \in \mathrm{Mod}(\Sigma_2)$ with the following conditions on each curve in $\mathfrak{S}_1$:

(1) φ is contained in the kernel of Φ_{c_3},
(2) φ maps the curve $t_{c_1}(c_2)$ to the curve $t_{c_4}(c_3)$.

It is easy to verify that the element $\varphi_0 = {t_x}^{-1} \cdot t_y \cdot {t_{c_1}}^{-1} \cdot t_{c_5}$ satisfies the above conditions, where x, y are curves in Σ_2 described in the right side of Figure 12. A surface diagram of the critical locus $\widetilde{s}_{1,2}$ is as follows:

$$\mathfrak{S}_{1,2} = (\Sigma_2; c_2, c_3, \varphi_0(c_2), t_{c_4}(c_3)).$$

We next connects $\widetilde{s}_{1,2}$ with s_3 by a cusp merge. We denote by $\widetilde{s}_{1,2,3}$ the resulting critical locus. The corresponding surgered surface diagram of $\widetilde{s}_{1,2,3}$ is obtained by changing a surgered surface diagram derived from the reference path γ_2^a (note that this path is now intersecting with the locus $\widetilde{s}_{1,2}$) so that the surgery disks and the path derived from $t_{c_4}(c_3)$ in this diagram match with the surgery disks and the path c in the surgered surface diagram derived from γ_3^b. As in the previous step, this modification is equivalent to applying an element $\psi \in \mathrm{Mod}(\Sigma_2)$ with the following conditions on each curve in $\mathfrak{S}_{1,2}$:

(3) ψ is contained in the kernel of Φ_{c_2},
(4) ψ maps the curve $t_{c_4}(c_3)$ to the curve $t_{c_1}(c_2)$.

It is easy to verify that the element $\psi_0 = t_{c_2}^{-2} \cdot {t_{c_5}}^{-1} \cdot t_z \cdot {t_{c_4}}^{-1} \cdot t_y$ satisfies the above conditions, where y, z are curves in Σ_2 described in the right side of Figure 12. A surface diagram of the critical locus $\widetilde{s}_{1,2,3}$ is as follows:

$$\mathfrak{S}_{1,2,3} = (\Sigma_2; c_3, c_2, \psi_0(c_3), \psi_0 \circ \varphi_0(c_2), t_{c_1}(c_2)).$$

To obtain simple wrinkled fibration on $E(n)$ we apply cusp merges successively as above. We denote by $\widetilde{s}_{1,2,\ldots,k}$ the singular locus obtained by connecting the loci $s_1, s_2, \ldots, s_k$ by the successive merges. By induction we can obtain the following surface diagram of this locus:

$$\begin{aligned}
\mathfrak{S}_{1,2,\ldots,2i-1} =& (\Sigma_2; c_3, c_2, \psi_0(c_3), \psi_0 \circ \varphi_0(c_2), \ldots \\
& \ldots, (\psi_0 \circ \varphi_0)^{i-2} \circ \psi_0(c_3), (\psi_0 \circ \varphi_0)^{i-1}(c_2), t_{c_1}(c_2)), \\
\mathfrak{S}_{1,2,\ldots,2i} =& (\Sigma_2; c_2, c_3, \varphi_0(c_2), \varphi_0 \circ \psi_0(c_3), \ldots \\
& \ldots, (\varphi_0 \circ \psi_0)^{i-1}(c_3), (\varphi_0 \circ \psi_0)^{i-1} \circ \varphi_0(c_2), t_{c_4}(c_3)).
\end{aligned}$$

In particular, a surface diagram of $E(n)$ is obtained as follows:

$$\begin{aligned}
\mathfrak{S}_{E(n)} =& (\Sigma_2; c_2, c_3, \varphi_0(c_2), \varphi_0 \circ \psi_0(c_3), \ldots \\
& \ldots, (\varphi_0 \circ \psi_0)^{6n-1}(c_3), (\varphi_0 \circ \psi_0)^{6n-1} \circ \varphi_0(c_2), t_{c_4}(c_3)).
\end{aligned}$$

5.2. **From Heegaard diagrams to surface diagrams.** In this subsection, we will explain an algorithm to obtain a surface diagram of $S^1 \times M^3$ from a Heegaard diagram of M^3 where M^3 is a closed, oriented, connected 3-manifold. Note that the corresponding simple wrinkled fibration on $S^1 \times M^3$ is null-homotopic. Indeed, it follows directly by construction that the fibration is homotopic to a map to S^2 which is not surjective.

Recall that a Heegaard diagram of M^3 is a triple $(\Sigma_g; \boldsymbol{\alpha}, \boldsymbol{\beta})$, where Σ_g is a closed, oriented surface of genus g, and $\boldsymbol{\alpha} = \{\alpha_1, \ldots, \alpha_g\}, \boldsymbol{\beta} = \{\beta_1, \ldots, \beta_g\}$ are g-tuples of mutually disjoint simple closed curves on Σ_g both of which are linearly independent in the homology group $H_1(\Sigma_g)$. A Heegaard diagram of M induces a handle decomposition of M and a Morse function $h_0 : M \to [-g-2, g+2]$. By perturbing h_0 we assume that the value of the index-0 (resp. 3) critical point is $-g-1$ (resp. $g+1$), and the value of the index-1 (resp. 2) critical point corresponding to α_i (resp. β_i) is $-g-1+i$ (resp. i). Such a map gives a stable map $\mathrm{id}_{S^1} \times h_0 : S^1 \times M \to S^1 \times [-g-2, g+2]$ over $S^1 \times M$. By collapsing the boundary of the annulus $S^1 \times [-g-2, g+2]$, we can obtain $f_0 : S^1 \times M \to S^2$ with two components of definite folds and $2g$ components of indefinite folds which are embedded into S^2 and have parallel images. Since the images of the two definite folds are the inner-most circles in the image $f_0(\mathcal{C}_{f_0})$, we can apply the deformation in Example 2 of [W1] to these definite folds. This deformation replaced the definite folds by indefinite ones (see Figure 13) and results in a surjective map and thus a wrinkled fibration $f_1 : S^1 \times M \to S^2$. We consider the two disks D_1, D_2 in the inner-most regions of the complements of $f_1(\mathcal{C}_{f_1})$ (the shaded disks in Figure 13).

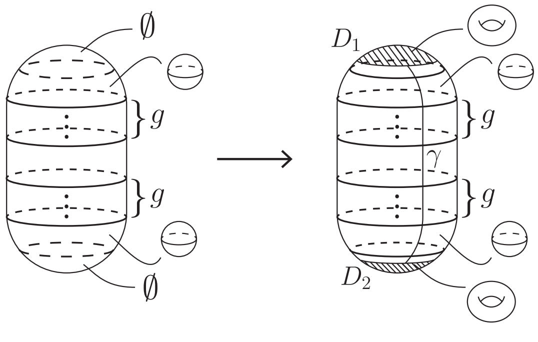

FIGURE 13. The left picture is the base diagram of the fibration f_0, and the right one is that of the fibration f_1.

Lemma 5.1. *Let $\gamma \subset S^2$ be the arc shown in Figure 13. There exists a commutative diagram*

$$\begin{tikzcd}
(S^1 \times M) \setminus \mathrm{Int}\big(f_1^{-1}(D_1) \amalg f_1^{-1}(D_2)\big) \arrow[r, "\Phi"] \arrow[d, "f_1"'] & S^1 \times f_1^{-1}(\gamma) \arrow[d, "\mathrm{id} \times h_1"] \\
S^2 \setminus \mathrm{Int}(D_1 \amalg D_2) \arrow[r, "\phi"] & S^1 \times I,
\end{tikzcd}$$

where Φ and ϕ are diffeomorphisms and h_1 is the restriction $f_1|_{f_1^{-1}(\gamma)}$.

Proof. Let B_i be a disk in S^2 which contains D_i and either of the inner-most images of folds, and is disjoint from the other images of folds of f_1. It is easy to see by construction of f_1 that there exist desired diffeomorphisms Φ and ϕ defined on $(S^1 \times M) \setminus \mathrm{Int}(f_1^{-1}(B_1) \amalg f_1^{-1}(B_2))$ and $S^2 \setminus \mathrm{Int}(B_1 \amalg B_2)$, respectively. This implies that we can identify $f_1^{-1}(\partial B_1) \amalg f_1^{-1}(\partial B_2)$ with $S^1 \times (f_1^{-1}(q_1) \amalg f_1^{-1}(q_2))$ in the natural way, where q_i is a point in $f_1^{-1}(B_i)$.

Next, we observe that the manifold $(S^1 \times M) \setminus \mathrm{Int}(f_1^{-1}(D_1) \amalg f_1^{-1}(D_2))$ is obtained from $(S^1 \times M) \setminus \mathrm{Int}(f_1^{-1}(B_1) \amalg f_1^{-1}(B_2))$ by a round 1-handle attachment (for a precise definition of round handles, see [B2], for example). This round 1-handle is untwisted and is attached with 0-framing since the monodromy of the higher-genus side of the inner-most fold is trivial by construction. Thus, we can identify $(S^1 \times M) \setminus \mathrm{Int}(f_1^{-1}(D_1) \amalg f_1^{-1}(D_2))$ with

$$(S^1 \times M) \setminus \mathrm{Int}\big(f_1^{-1}(B_1) \amalg f_1^{-1}(B_2)\big) \cup_{\mathrm{id}_{S^1} \times (\psi_1 \amalg \psi_2)} \big((S^1 \times D^1 \times D^2) \amalg (S^1 \times D^1 \times D^2)\big)$$

where $\psi_i : \partial D^1 \times D^2 \to f_1^{-1}(q_i)$ is an embedding which is independent of S^1-parameter. This implies the statement in Lemma 5.1. □

Lemma 5.1 guarantees that we can move the inner-most folds to the middle region as described in Figure 14. By the end of the deformation the genus of a fiber of the middle region is $g + 2$. We denote by $f_2 : S^1 \times M \to S^2$ the fibration obtained by this deformation, and by $a_1, \ldots, a_{g+1}, b_1, \ldots, b_{g+1}$ the images of folds as described in Figure 14.

To obtain a simple wrinkled fibration on $S^1 \times M$, we next apply the flip and slip to the folds a_1 and b_1 of f_2. We denote the modified folds with four cusps by $\widetilde{a_1}$

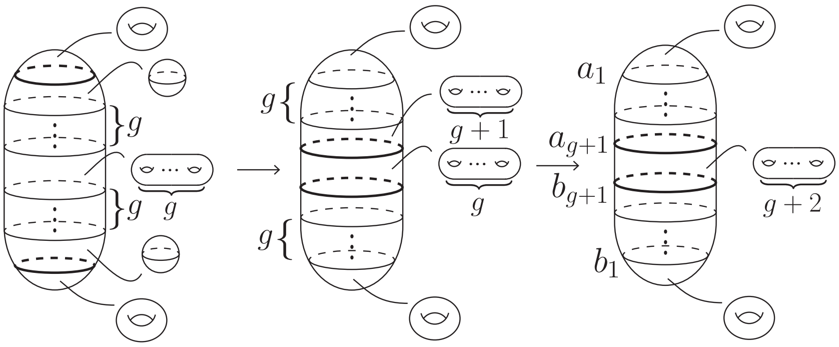

Figure 14. The far left figure describes a base diagram of f_1, while the far right one describes that of f_2. We first move the inner-most folds (the bold circles in the figure) to the middle region. Then, we interchange these folds so that the middle region has the highest genus fibers.

and $\widetilde{b_1}$. These folds can be moved to the middle region as described in the center of Figure 15. After the above deformations, we can next apply the flip and slip to the inner-most folds a_2 and b_2, and the modified folds $\widetilde{a_2}$, $\widetilde{b_2}$ can be moved to the middle region. By successive application of the same moves, the fibration ends up having $2g+2$ circular singularities each of which has four cusps (see Figure 15). We denote this fibration by $f_3 : S^1 \times M \to S^2$.

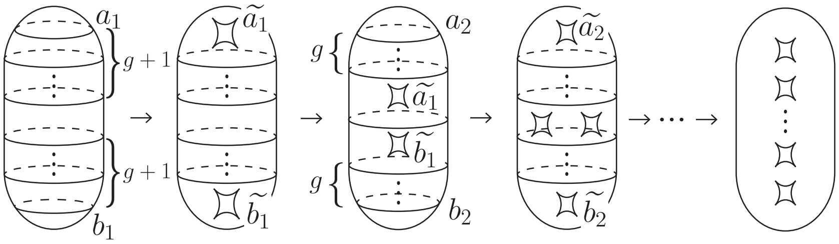

Figure 15. Successive application of flip and slips. The far left figure is a base diagram of f_2, while the far right one is that of f_3.

A simple wrinkled fibration over $S^1 \times M$ can be obtained by applying cusp merges to f_3 to make the critical set connected. We need to know a surgered surface diagram of each component $\widetilde{a_i}$ and $\widetilde{b_i}$ to obtain a corresponding surface diagram. As explained in the previous paragraph, the fibration f_3 is obtained by successive application of flip and slips followed by isotopy deformations which moves inner-most folds to the middle region. We can obtain a surgered surface diagram of each component $\widetilde{a_i}$ and $\widetilde{b_i}$ once we know that of the corresponding inner-most fold. Indeed, surgered surface diagrams of $\widetilde{a_i}$ and $\widetilde{b_i}$ are nothing but lifts of the corresponding inner-most folds.

The first flip and slips are applied to folds a_1 and b_1, whose lower-genus fibers are tori. According to the result in [H2], to obtain surgered surface diagrams of $\widetilde{a_1}$ and $\widetilde{b_1}$, we have to look at not only monodromies of the higher-genus sides of a_1 and b_1, but also sections over disks B_i $(i = 1, 2)$ which contain D_i and either of the images a_1 or b_1 and are disjoint from the other images of $\mathcal{C}_{f_1}$. By Lemma 5.1 the monodromy of the higher-genus side is trivial. Furthermore, we can identify

$S^1 \times M$ as the following manifold:

$$S^1 \times f_1^{-1}(\gamma) \cup_{\varphi_1 \amalg \varphi_2} (D_1 \times T^2 \amalg D_2 \times T^2),$$

where $\varphi_i : \partial D_i \times T^2 \to S^1 \times \partial f^{-1}(\gamma)$ is a gluing diffeomorphism. By identifying $\partial f_1^{-1}(\gamma)$ with a pair of tori we can regard φ_i as a self-diffeomorphism of $S^1 \times T^2$. Note that we understand the behavior of the sections over B_1 and B_2 once we know the maps φ_1 and φ_2. Thus, the following lemma enables us to obtain surgered surface diagrams of $\widetilde{a_1}$ and $\widetilde{b_1}$.

Lemma 5.2. *For a suitable identification $\partial f_1^{-1}(\gamma) \cong T^2 \amalg T^2$, there exists an embedding $\theta : S^1 \to T^2$ whose image intersects a vanishing cycle of the fold in one point such that the restriction $\varphi_i|_{S^1 \times \{*\}}$ is isotopic to the following map:*

$$S^1 \ni z \mapsto (z, \theta(z)) \in S^1 \times T^2.$$

Proof. Let H_1 be a solid torus. We take a small ball B^3 in the interior $\mathrm{Int}(H_1)$. By Lemma 5.1, we can identify $f_1^{-1}(B_i \setminus \mathrm{Int}(D_i))$ with $S^1 \times (H_1 \setminus B^3)$. Thus, we can regard $f_1^{-1}(B_i)$ as the manifold obtained by attaching $D^2 \times T^2$ to $S^1 \times (H_1 \setminus B^3)$. Such a manifold is well-studied in the proof of Theorem 4.2 of [H1]. It is easy to see by construction of f_1 that the manifold $f_1^{-1}(B_i)$ is diffeomorphic to $S^1 \times S^3$. This diffeomorphism, together with the argument in [H1], implies that the attaching map φ_i satisfies the condition in the statement. □

The other flip and slips are applied to folds over a_i and b_i ($i \geq 2$) whose lower genus fibers have genus two or higher. Thus, in these cases, we can obtain surgered surface diagrams of $\widetilde{a_i}$ and $\widetilde{b_i}$ once we know the monodromies of the higher-genus sides of a_i and b_i. These monodromies are no longer trivial, yet we can easily obtain them by looking at lifts of surgered diagrams of the previous folds $\widetilde{a_{i-1}}$ and $\widetilde{b_{i-1}}$ (see also the examples below).

Example 5.3. We first look at the simplest example: the genus-0 Heegaard diagram $(S^2, \boldsymbol{\alpha} = \boldsymbol{\beta} = \emptyset)$ of S^3. We denote by $f_i \colon S^1 \times S^3 \to S^2$, $i = 0, \ldots, 3$ the maps obtained in the various steps of the algorithm explained above. Since there are no curves in the Heegaard diagram, it is easy to obtain a surgered surface diagram of f_1 which is described in Figure 16. The fibration f_2 is obtained from f_1 by moving the folds so that the middle region has the highest genus fibers. We can also obtain a surgered surface diagram of f_2, which is also described in Figure 16.

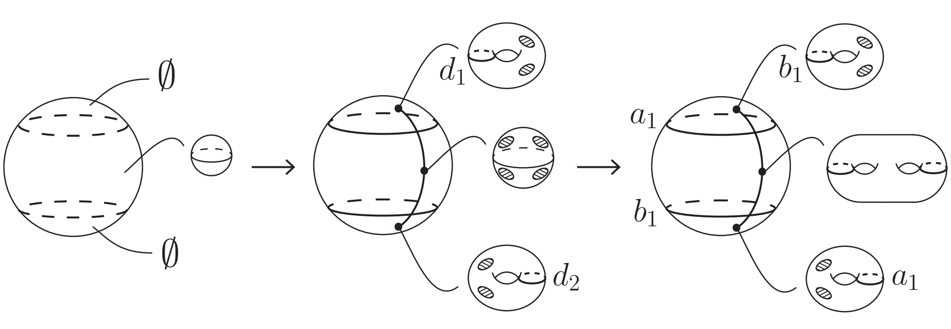

FIGURE 16. The right figure is a base diagram of f_0. The bold circles are images of definite folds. The middle one is that of f_1 with surgered diagrams, and the left one is that of f_2. We also denote by a_1 and b_1 vanishing cycles of folds a_1 and b_1, respectively. The shaded disks describe surgery disks.

We next apply flip and slips to the folds a_1 and b_1 of f_2. We take sections of f_2 over disks B_1 and B_2, where B_i is a disk in S^2 whose interior contains one of the lower-genus regions (as in the argument above). These sections provide lifts of the monodromies of the higher-genus sides of the folds a_1 and b_1 to the mapping class group with a marked point x. It is easy to verify that we can choose a homotopy from f_0 to f_2 and sections so that the monodromy along a_1 (resp. b_1) is equal to the pushing map along θ_1 (resp. θ_2), where θ_i is an oriented loop described in the left side of Figure 17. We denote by Σ_1 a regular fiber of f_3 whose image is contained in the inside of $\widetilde{a_1}$. We take simple closed curves θ_1^+ and θ_1^- in Σ_1 as described in the left side of Figure 18 and put $\varphi_1 = t_{\theta_1^+} t_{\theta_1^-}^{-1} \in \mathrm{Mod}(\Sigma_1)$. According to the argument in [H2], a surface diagram derived from the critical set $\widetilde{a_1}$ is as follows:

$$\mathfrak{S}_a = (\Sigma_1; d_1, \varphi_1^{-1}(\delta_1), a_1, \delta_1),$$

where δ_1 and d_1 are the simple closed curves in Σ_1 described in the right side of Figure 17. Similarly, we denote by Σ_2 a regular fiber of f_3 whose image is contained in the inside of $\widetilde{b_1}$ and consider simple closed curves $\theta_2^{\pm}$ as described in the right side of Figure 18. A surface diagram derived from the critical set $\widetilde{b_1}$ is as follows:

$$\mathfrak{S}_b = (\Sigma_2; e_1, \epsilon_1, b_1, \varphi_2^{-1}(\epsilon_1)),$$

where e_1 and ϵ_1 are the curves described in the right side of Figure 17.

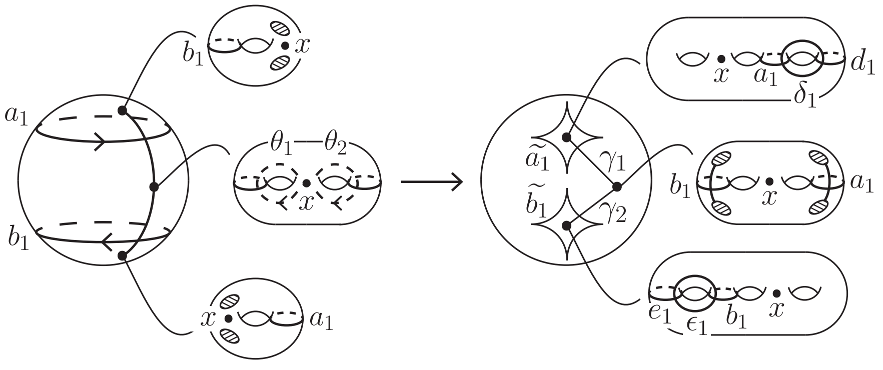

FIGURE 17. The left figure is a base diagram of f_2, while the right one is that of f_3. The shaded disks describe surgery disks derived from the paths γ_1 and γ_2.

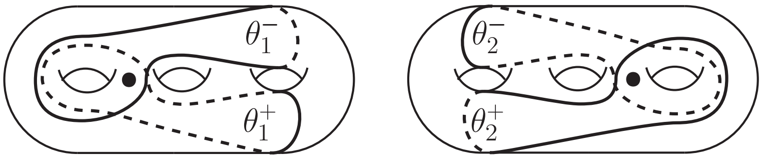

FIGURE 18. Left: simple closed curves in Σ_1. Right: those in Σ_2.

We consider arcs γ_1 and γ_2 in S^2 as in the right side of Figure 17. We denote by Σ_0 the fiber on the intersection between γ_1 and γ_2. These paths give surgered surface diagrams which are described in Figure 19. We denote these diagrams by $\mathfrak{S}'_a$ and $\mathfrak{S}'_b$. To obtain a surface diagram of the fibration after applying a cusp merge we change the diagram $\mathfrak{S}'_b$ by an isotopy of Σ_0 (as described in Figure 19) so that the surgery disks and the arc ϵ_1 in $\mathfrak{S}'_b$ coincide with the surgery disks and the arc δ_1 in $\mathfrak{S}'_a$. We denote by $\widehat{b_1}$, $\widehat{\epsilon_1}$ and $\widehat{\varphi_2^{-1}(\epsilon_1)}$ the curves and arcs in Σ_0 obtained after applying the above modification to b_1, ϵ_1 and $\varphi_2^{-1}(\epsilon_1)$, respectively. We can regard $\widetilde{b_1}$ and $\widehat{\varphi_2^{-1}(\epsilon_1)}$ as simple closed curves in Σ_1. Note that the curve $\widehat{\varphi_2^{-1}(\epsilon_1)}$ is equal to $\varphi_1^{-1}(\delta_1)$. By the argument in the beginning of Section 5 we eventually obtain the following surface diagram of $S^1 \times S^3$:

$$(\Sigma_1; d_1, \varphi_1^{-1}(\delta_1), a_1, \delta_1, \widehat{b_1}, \varphi_1^{-1}(\delta_1)),$$

which is shown in Figure 20.

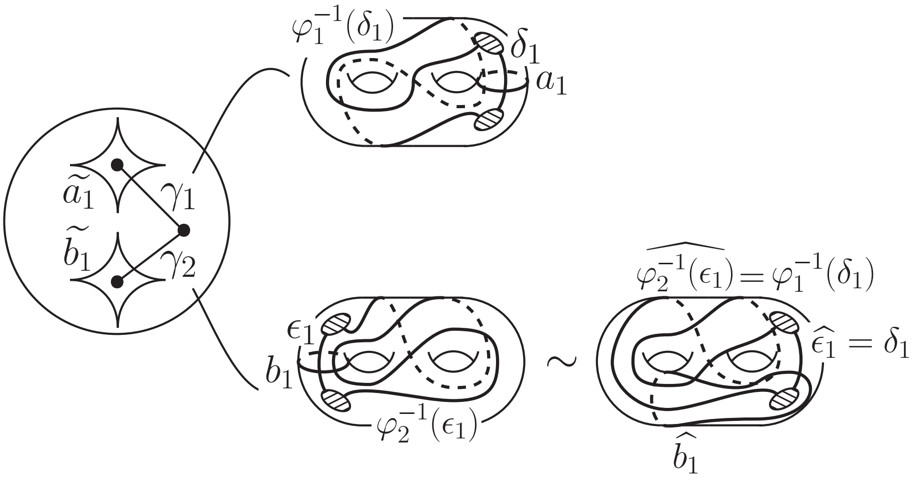
$\varphi_1^{-1}(\delta_1)$
δ_1
a_1
$\widetilde{a_1}$
γ_1
$\widetilde{b_1}$
γ_2
$\widehat{\varphi_2^{-1}(\epsilon_1)} = \varphi_1^{-1}(\delta_1)$
ϵ_1
b_1
$\sim$
$\widehat{\epsilon_1} = \delta_1$
$\varphi_2^{-1}(\epsilon_1)$
$\widehat{b_1}$

FIGURE 19. The surgered surface diagrams $\mathfrak{S}'_a$ (on top) and $\mathfrak{S}'_b$ (on the bottom).

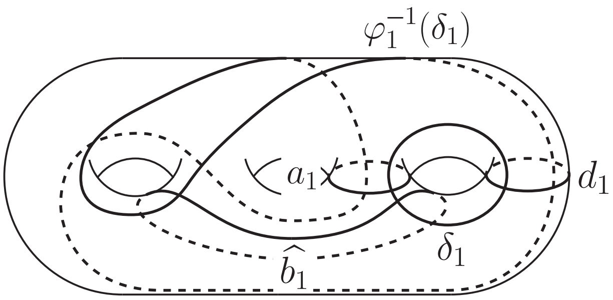

FIGURE 20. A surface diagram of $S^1 \times S^3$ derived from the genus-0 Heegaard diagram.

Example 5.4. We next construct a surface diagram of $S^1 \times L(p,1)$ derived from the standard genus-1 Heegaard diagram of $L(p,1)$ shown in Figure 21. As in Example 5.3 we denote the fibrations $S^1 \times L(p,1) \to S^2$ obtained in the steps of our algorithm by f_i, $i = 0, \ldots, 3$. The fibration f_2 has four parallel indefinite folds a_1,a_2, b_1 and b_2 and corresponding vanishing cycles are shown in the left side of Figure 22. As in Example 5.3 we can choose a homotopy from f_0 to f_2 so that a lifted monodromy along a_1 (resp. b_1) is equal to the pushing map along an oriented loop θ_1 (resp. θ_2) described in the left side of Figure 22. To obtain the fibration f_3 from f_2 we first apply flip and slips to the folds a_1 and b_1, which are changed into $\widetilde{a_1}$ and $\widetilde{b_1}$,

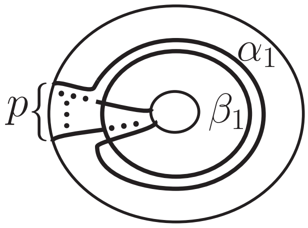

FIGURE 21. A Heegaard diagram of $L(p, 1)$.

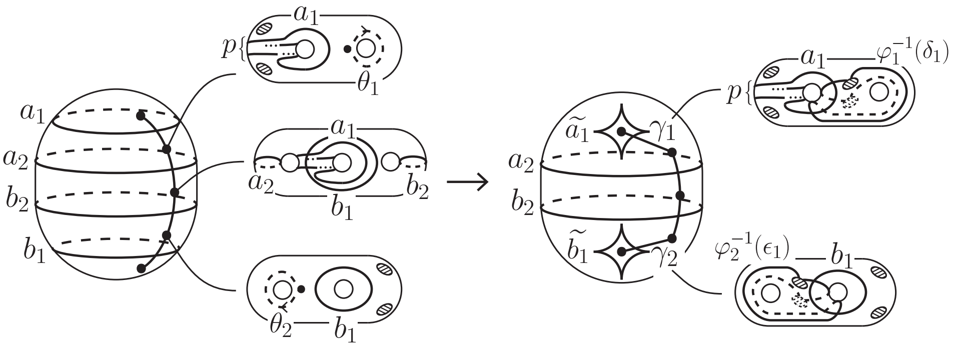

FIGURE 22. Left: surgered diagrams of f_2. Right: those of the fibration obtained after applying the first flip and slips.

respectively. We take reference arcs γ_1 and γ_2 as described in the right side of Figure 22. We also take simple closed curves $\theta_1^{\pm}, \theta_2^{\pm}$ as described in Figure 23. Note

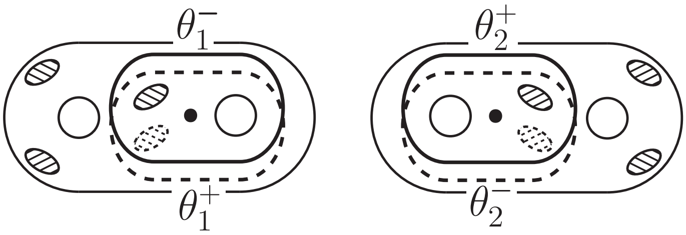

FIGURE 23. Simple closed curves in surgered diagrams.

that these simple closed curves can be regarded as curves in higher genus fibers in the natural way. We put $\varphi_1 = t_{\theta_1^+} t_{\theta_1^-}^{-1}$ and $\varphi_2 = t_{\theta_2^+} t_{\theta_2^-}^{-1}$. By the same argument as in [H2] we can obtain surgered diagrams derived from a reference path γ_i which is described in the right side of Figure 22.

After moving the singular loci $\widetilde{a_1}$ and $\widetilde{b_1}$ into the middle region, we next apply flip and slips to a_2 and b_2 as in Figure 24. We take reference paths γ_3 and γ_4 as described in the far right of Figure 24. To obtain a surgered diagram derived from γ_3 we need to look at the monodromy of the higher side of a_2. By Lemma 5.1 this monodromy is equal to the monodromy which appears when we go around $\widetilde{a_1}$ clockwise. Thus, the monodromy of the higher side of a_2 is calculated as follows:

$$
\begin{aligned}
&\Phi_{d_1}\left(\{t_{t_{\delta_1}(d_1)} t_{t_{a_1}(\delta_1)} t_{t_{\varphi_1^{-1}(\delta_1)}(a_1)} t_{t_{d_1}(\varphi_1^{-1}(\delta_1))}\}^{-1}\right) \\
=&\Phi_{d_1}\left(t_{d_1} t_{\varphi_1^{-1}(\delta_1)}{}^{-1} t_{d_1}{}^{-1} t_{\varphi_1^{-1}(\delta_1)} t_{a_1}{}^{-1} t_{\varphi_1^{-1}(\delta_1)}{}^{-1} t_{a_1} t_{\delta_1}{}^{-1} t_{a_1}{}^{-1} t_{\delta_1} t_{d_1}{}^{-1} t_{\delta_1}{}^{-1}\right)
\end{aligned}
$$

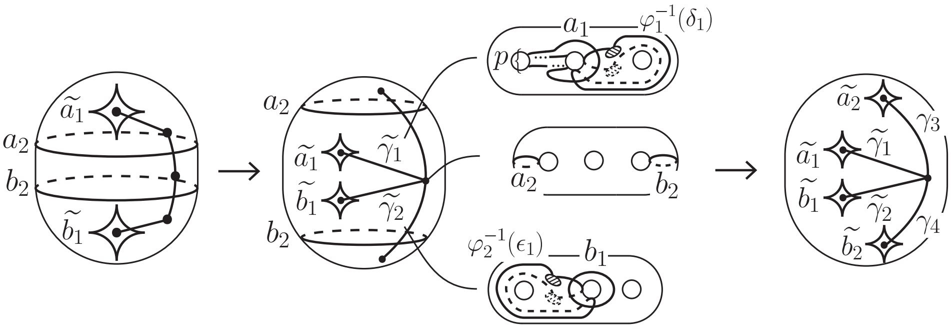

FIGURE 24. A homotopy which moves the critical loci with cusps to the middle region followed by the second flip and slips.

$$\begin{aligned}
&=\Phi_{d_1}\left(t_{d_1}\right)\Phi_{d_1}\left(t_{\varphi_1^{-1}(\delta_1)}{}^{-1}t_{d_1}{}^{-1}t_{\varphi_1^{-1}(\delta_1)}{}^{2}t_{a_1}{}^{-1}t_{\varphi_1^{-1}(\delta_1)}{}^{-1}t_{\delta_1}{}^{-1}t_{a_1}{}^{-1}t_{d_1}{}^{-1}t_{\delta_1}{}^{-1}t_{d_1}\right)\\
&=\Phi_{d_1}\left(t_{d_1}{}^{2}t_{\varphi_1^{-1}(\delta_1)}{}^{-1}t_{d_1}{}^{-1}t_{a_1}{}^{-1}t_{\varphi_1^{-1}(\delta_1)}{}^{-1}t_{\delta_1}{}^{-1}t_{a_1}{}^{-1}t_{d_1}{}^{-1}t_{\delta_1}{}^{-1}\right)\\
&=\Phi_{d_1}\left(\varphi_1{}^{-1}t_{\delta_1}{}^{-1}\varphi_1 t_{d_1}{}^{-1}t_{a_1}{}^{-1}\varphi_1^{-1}t_{\delta_1}{}^{-1}\varphi_1 t_{\delta_1}{}^{-1}t_{a_1}{}^{-1}t_{d_1}{}^{-1}t_{\delta_1}{}^{-1}\right)\\
&=\Phi_{d_1}\left(t_{\delta_1}{}^{-1}t_{d_1}{}^{-1}t_{a_1}{}^{-1}t_{\delta_1}{}^{-1}\varphi_1 t_{\delta_1}{}^{-1}t_{a_1}{}^{-1}t_{d_1}{}^{-1}t_{\delta_1}{}^{-1}\right)\\
&=\Phi_{d_1}\left(\Theta_a\varphi_1\Theta_a{}^{-1}\Theta_a{}^{2}\right)\\
&=\Phi_{d_1}\left(\Theta_a\varphi_1\Theta_a{}^{-1}\right),
\end{aligned}$$

where we put $\Theta_a = t_{\delta_1}{}^{-1}t_{d_1}{}^{-1}t_{a_1}{}^{-1}t_{\delta_1}{}^{-1} = t_{\delta_1}{}^{-1}t_{a_1}{}^{-1}t_{d_1}{}^{-1}t_{\delta_1}{}^{-1}$, and the last equality holds since the element $\Theta_a{}^2$ is contained in the kernel of Φ_{d_1}. We take simple closed curves $\theta_3^{\pm}$, $\widetilde{\theta_3^{\pm}}$ and $\widetilde{\theta_4^{\pm}}$ as described in Figure 25. It is easy to verify

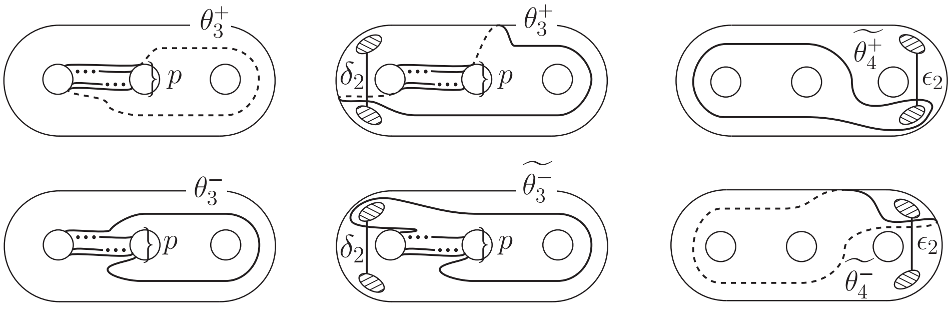

FIGURE 25. Simple closed curves $\theta_3^{\pm}$, $\widetilde{\theta_3^{\pm}}$ and $\widetilde{\theta_4^{\pm}}$. Note that the curve $\widetilde{\theta_3^{\pm}}$ is a lift of $\theta_3^{\pm}$.

that the element $\Phi_{d_1}(\Theta_a\varphi_1\Theta_a{}^{-1})$ coincides with the product $t_{\theta_3^+}t_{\theta_3^-}^{-1}$. We denote by δ_2 a simple closed curve in genus-4 surface Σ which corresponds to the arc described in Figure 25 under the surgery and by d_2 a simple closed curve in Σ which is parallel to the boundary of a surgered region. According to the argument in [H2], a surface diagram derived from the critical set $\widetilde{a_2}$ is as follows:

$$\mathfrak{S}_{a_2} = (\Sigma; d_2, \varphi_3^{-1}(\delta_2), a_2, \delta_2),$$

where we put $\varphi_3 = t_{\widetilde{\theta_3^+}}t_{\widetilde{\theta_3^-}}^{-1}$. In a similar way, we can also obtain the following surface diagram derived from the critical set $\widetilde{b_2}$:

$$\mathfrak{S}_{b_2} = (\Sigma'; e_2, \epsilon_2, b_2, \varphi_4^{-1}(\epsilon_2)),$$

where Σ' is a genus-4 surface obtained by the surgery from the surface described in the far right side of Figure 25, ϵ_2 is a simple closed curve in Σ' derived from the arc described in Figure 25, e_2 is a simple closed curve in Σ' which is parallel to the boundary of a surgered region, and φ_4 is defined as the product $t_{\widetilde{\theta_4^+}} t^{-1}_{\widetilde{\theta_4^-}}$.

The remaining procedure to obtain a genus-4 surface diagram of $S^1 \times L(p,1)$ is tedious. We only give a resulting surface diagram $(\Sigma_4; c_1, \ldots, c_{10})$, where the curves in this diagram are described in Figure 26, and leave the details of the procedure to the readers.

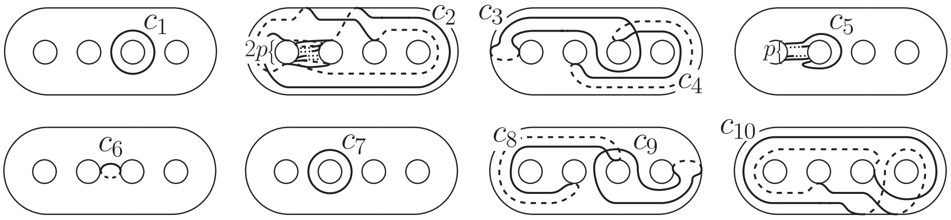

FIGURE 26. Curves in a surface diagram of $S^1 \times L(p,1)$.

5.3. **Boundary fiber sums.** Suppose that we are given two surjective smooth maps $f_i \colon X_i \to D_i$, $i = 1, 2$, onto oriented disks D_i such that two regular fibers over the boundaries are diffeomorphic. Then we can glue the maps together as follows. We first choose orientation preserving embeddings of a small interval $(-\epsilon, \epsilon)$ into the regular part of ∂D_i where we have diffeomorphic fibers and glue D_2 to D_1 along the images with the map that sends s to $-s$ to obtain a new disk $D_1 \natural D_2$. Next, we choose an orientation preserving diffeomorphism $\phi' \colon f_2^{-1}(0) \to f_1^{-1}(0)$ and form a 4–manifold $X_1 \natural_\phi X_2$ by gluing X_1 and X_2 along $f_1^{-1}(-\epsilon, \epsilon)$ and $f_2^{-1}(-\epsilon, \epsilon)$, which we identify with $f_i^{-1}(p_i) \times (-\epsilon, \epsilon)$, using the diffeomorphism that sends (p, s) to $(\phi'(p), -s)$. This constructions also produces an obvious map denoted by

$$f_1 \natural_{\phi'} f_2 \colon X_1 \natural_{\phi'} X_2 \to D_1 \natural D_2$$

which is called the *boundary fiber sum of* f_1 *and* f_2 *along* ϕ'. For brevity of notation we will tacitly assume in the following that all disks that arise as the base of some fibration are normalized to the standard disk D^2.

If we apply this construction to simple wrinkled fibrations $w_i \colon X_i \to D^2$, then we obtain a wrinkled fibration $w_1 \natural_{\phi'} w_2$ whose critical image consists of two disjointly embedded circles with cusps facing the boundary. We can turn this map into a simple wrinkled fibration by joining the two circles with a cusp merge. We will call any simple wrinkled fibration obtained in this way as a *merged boundary fiber sum.* Our goal is to obtain a interpretation of this construction in terms of surface diagrams. Throughout the discussion we fix the simple wrinkled fibrations w_i and denote their surface diagrams by $\mathfrak{S}_1 = (\Sigma_1; c_1, \ldots, c_k)$ and $\mathfrak{S}_2 = (\Sigma_2; d_1, \ldots, d_l)$.

It is clear, that the effect of a merged boundary sum must be of the following form. There is a diffeomorphism $\phi \colon \Sigma_2 \to \Sigma_1$ with the property that $\phi(d_1)$ is isotopic to c_k and $\phi(d_l)$ is isotopic to c_1, and the surface diagram is given by

$$\mathfrak{S}_1 \natural_\phi \mathfrak{S}_2 := \big(\Sigma_1; c_1, \ldots, c_k, \phi(d_2), \ldots, \phi(d_{l-1})\big). \tag{5.1}$$

This operation clearly makes sense for abstract surface diagrams and we will say that $\mathfrak{S}_1 \natural_\phi \mathfrak{S}_2$ is a *fusion* of $\mathfrak{S}_1$ and $\mathfrak{S}_2$. As we will presently see, any fusion of $\mathfrak{S}_1$ and $\mathfrak{S}_2$ describes some merged boundary fiber sum of $w_1 \natural_{\phi'} w_2$. What is not clear, however, is the relation between ϕ and ϕ'.

To understand this, we identify Σ'_i as the surgery on $c_k \subset \Sigma_1$, resp. on $d_1 \subset \Sigma_2$ by choosing reference arcs from the images of Σ_i in D^2 to the image of Σ'_i which cross the respective critical images in the fold arcs corresponding to c_k and d_1. However, since the lower genus regions are half-open annuli, there are no canonical choices of reference paths and the resulting identifications might not be unique, not even up to isotopy. In fact, up to isotopy the difference for each identification is measured by powers of the *boundary monodromy* of w_i, ie the mapping class $\mu_i \in \operatorname{Mod}(\Sigma'_i)$ obtained by the parallel transport once around the boundary of the disk in a counterclockwise manner.

Now consider the fusion $\mathfrak{S}_1 \natural_\phi \mathfrak{S}_2$ as in (5.1). For simplicity we assume that the pairs of vanishing cycles (c_k, c_1) and (d_1, d_l) are in minimal position and that ϕ satisfies $\phi(d_1) = c_k$ and $\phi(d_l) = c_1$. Then ϕ induces a diffeomorphism from the surgery on $d_1 \subset \Sigma_2$ to the surgery on $c_k \subset \Sigma_1$. If we identify some boundary fibers Σ'_i of w_i with these surgered surfaces by choosing reference arcs as above, then we obtain a diffeomorphism $\phi'_0 \colon \Sigma'_2 \to \Sigma'_1$ which we can use to form a boundary fiber sum $w_1 \natural_{\phi'_0} w_2$. In $w_1 \natural_{\phi'_0} w_2$ the former boundary fibers Σ'_i appear as a single fiber Σ' and the reference arcs induce surgered surface diagrams for both w_1 and w_2. Since ϕ also maps d_l to c_1, these diagrams are already matched for a cusp merge between the cusps with vanishing cycles (c_k, c_1) and (d_1, d_l) along the obvious cusp merge arc obtained by pushing the reference arcs into the cusps. More or less by definition of ϕ'_0 the resulting identification of the higher genus fibers is given by ϕ, so that the surface diagram of the merged boundary fiber sum is $\mathfrak{S}_1 \natural_\phi \mathfrak{S}_2$. If we used the same boundary fibers but difference reference arcs, then we would obtain different diffeomorphisms between the boundary fibers which would be of the form $\phi'_{mn} = \mu_1^m \phi_0 \mu_2^n$. Thus the surface diagram $\mathfrak{S}_1 \natural_\phi \mathfrak{S}_2$ can arise in more then one way from a merged boundary fiber sum. Note however, that the wrinkled fibrations $w_1 \natural_{\phi'_{m,n}} w_2$ are all homotopic. In fact, they differ by a sequence of generalized shift deformations.

Next, given a boundary fiber sum $w_1 \natural_{\phi'} w_2$, we want to determine which surface diagrams can be obtained by merging the cusps with vanishing cycles (c_k, c_1) and (d_1, d_l). We again identify the fiber Σ' coming from the former boundary fibers with the surgeries on c_k and d_1 to obtain surgered surface diagrams for the w_i in Σ'. This time, however, the surgered surface diagrams are not automatically matched for a cusps merge and we have to choose a matching isotopy. A choice of matching isotopy then leads to a diffeomorphism $\phi_0 \colon \Sigma_2 \to \Sigma_1$ and the merged boundary fiber sum derived from these choices will be $\mathfrak{S}_1 \natural_{\phi_0} \mathfrak{S}_2$. There is a twofold ambiguity for ϕ_0 caused by the choices of matching isotopies and reference arcs. By the results of Section 3, we know that choosing a different matching isotopy corresponds to composing ϕ_0 with an element of $\ker \Phi_{c_1} \cap \ker \Phi_{c_k}$. In order to describe the dependence on the reference path we represent the boundary monodromies μ_i be diffeomorphisms that fix the surgery disks and the arcs c'_1 and d'_l. We then obtain a diffeomorphisms of Σ_i which represent mapping classes $\tilde{\mu}_i \in \operatorname{Mod}(\Sigma_i)$. Note that the ambiguity of choosing the representatives for μ_i can be subsumed in the ambiguity of the matching isotopy. Altogether, the surface diagrams we obtain from $w_1 \natural_{\phi'} w_2$ are all of the form $\mathfrak{S}_1 \natural_\phi \mathfrak{S}_2$ where $\phi = \tilde{\mu}_1^m \xi \phi_0 \tilde{\mu}_2^n$ for some $\xi \in \ker \Phi_{c_1} \cap \ker \Phi_{c_k}$.

Recall that a surface diagram comes from a simple wrinkled fibration over the sphere if and only if it has *trivial monodromy*, that is, the boundary monodromy of the associated simple wrinkled fibration over the disk is trivial. An easy but important observation is the following.

Lemma 5.5. *Let w_1 and w_2 be simple wrinkled fibrations over the disk with boundary monodromy $\mu_i \in \operatorname{Mod}(\Sigma'_i)$ where Σ'_i is a boundary fiber of w_i. If $\phi \colon \Sigma'_2 \to \Sigma'_1$ is a diffeomorphism, then $w_1 \natural_{\phi'} w_2$ has boundary monodromy $\phi' \mu_2 \phi'^{-1} \mu_1 \in \operatorname{Mod}(\Sigma'_1)$.*

Corollary 5.6. *The fusion of surface diagrams preserves trivial monodromy. More precisely, if* $\mathfrak{S}_1$ *and* $\mathfrak{S}_2$ *have trivial monodromy, then any fusion* $\mathfrak{S}_1 \natural_\phi \mathfrak{S}_2$ *also has trivial monodromy.*

As a consequence, the fusion of surface diagrams can be interpreted as an operation on closed 4–manifolds, namely the fiber sum of simple wrinkled fibrations over the sphere taken along the lower genus fibers.

Acknowledgments. This work was carried out while the second author was visiting the Max Planck Institute for Mathematics in the summer of 2012. The authors would like to express their gratitude to Jonathan Williams for helpful comments and discussions. The first author was supported by an IMPRS Scholarship of the Max-Planck-Society. The second author was supported by JSPS Research Fellowships for Young Scientists (24·993).

References

- [B1] R. İnanç Baykur, *Existence of broken Lefschetz fibrations*, Int. Math. Res. Not. IMRN (2008), Art. ID rnn 101, 15.
- [B2] ———, *Topology of broken Lefschetz fibrations and near-symplectic four-manifolds*, Pacific J. Math. **240** (2009), no. 2, 201–230.
- [B3] Stefan Behrens, *On 4-manifolds, folds and cusps* (2012), available at `http://arxiv.org/abs/1205.5192`.
- [FM] Benson Farb and Dan Margalit, *A Primer on Mapping Class Groups*, Princeton Mathematical Series, vol. 49, Princeton University Press, Providence, RI, 2011.
- [GK1] David T. Gay and Robion Kirby, *Indefinite Morse 2-functions; broken fibrations and generalizations* (2011), available at `arXiv:1102.0750v2[math.GT]`.
- [GK2] ———, *Reconstructing 4-manifolds from Morse 2-functions* (2012), available at `http://de.arxiv.org/abs/1202.3487`.
- [H1] Kenta Hayano, *On genus-1 simplified broken Lefschetz fibrations*, Algebr. Geom. Topol. **11** (2011), no. 3, 1267–1322.
- [H2] ———, *Modification rule of monodromies in* R_2*-move* (2012), available at `http://de.arxiv.org/abs/1203.4299v1`.
- [L] Yanki Lekili, *Wrinkled fibrations on near-symplectic manifolds*, Geom. Topol. **13** (2009), no. 1, 277–318. Appendix B by R. İnanç Baykur.
- [W1] Jonathan Williams, *The h-principle for broken Lefschetz fibrations*, Geom. Topol. **14** (2010), no. 2, 1015–1061.
- [W2] ———, *Uniqueness of surface diagrams of smooth 4-manifolds* (2011), available at `http://arxiv.org/abs/1103.6263`.

Max Planck Institute for Mathematics, Bonn, Germany
E-mail address: `sbehrens@mpim-bonn.mpg.de`

Department of Mathematics, Graduate School of Science, Osaka University, Toyonaka, Osaka 560-0043, Japan
E-mail address: `k-hayano@cr.math.sci.osaka-u.ac.jp`